Molecular & Biochemical Parasitology 162 (2008) 1–15

Contents lists available at ScienceDirect

Molecular & Biochemical Parasitology

Alternative splicing: A novel mechanism of regulation identified in the chorismate mutase gene of the potato cyst nematode *Globodera rostochiensis*☆

Shun-Wen Lu[a], Duanhua Tian[a,1], Harmony B. Borchardt-Wier[b], Xiaohong Wang[a,b,*]

[a] *Department of Plant Pathology and Plant-Microbe Biology, Cornell University, Ithaca, NY 14853, USA*
[b] *USDA-ARS, Robert W. Holley Center for Agriculture and Health, Ithaca, NY 14853, USA*

ARTICLE INFO

Article history:
Received 17 December 2007
Received in revised form 13 May 2008
Accepted 3 June 2008
Available online 22 August 2008

Keywords:
Alternative splicing
Chorismate mutase
Globodera rostochiensis
Plant–parasitic nematode
Intron retention
Dominant negative isoform

ABSTRACT

Chorismate mutase (CM) secreted from the stylet of plant–parasitic nematodes plays an important role in plant parasitism. We isolated and characterized a new nematode *CM* gene (*Gr-cm-1*) from the potato cyst nematode, *Globodera rostochiensis*. The *Gr-cm-1* gene was found to exist in the nematode genome as a single-copy gene that has two different alleles, *Gr-cm-1A* and *Gr-cm-1B*, both of which could give rise to two different mRNA transcripts of *Gr-cm-1* and *Gr-cm-1-IRII*. *In situ* mRNA hybridization showed that the *Gr-cm-1* gene was exclusively expressed within the subventral oesophageal gland cells of the nematode. *Gr-cm-1* was demonstrated to encode a functional CM (GR-CM-1) potentially having a dimeric structure as the secreted bacterial *AroQ CMs. *Gr-cm-1-IRII*, generated by retention of intron 2 of the *Gr-cm-1* pre-mRNA through alternative splicing (AS), would encode a truncated protein (GR-CM-1t) lacking the CM domain with no CM activity. The quantitative real-time reverse transcription-PCR assay revealed that splicing of the *Gr-cm-1* gene was developmentally regulated; *Gr-cm-1* was up-regulated whereas *Gr-cm-1-IRII* was down-regulated in early nematode parasitic stages compared to the preparasitic juvenile stage. Low-temperature SDS-PAGE analysis revealed that GR-CM-1 could form homodimers when expressed in *Escherichia coli* and the dimerization domain was retained in the truncated GR-CM-1t protein. The specific interaction between the two proteins was demonstrated in yeast. Our data suggested that the novel splice variant might function as a dominant negative isoform through heterodimerization with the full-length GR-CM-1 protein and that AS may represent an important mechanism for regulating CM activity during nematode parasitism.

1. Introduction

Alternative splicing (AS) of precursor messenger RNA (pre-mRNA), a process allowing multiple mRNA transcripts to be generated from a single gene, is an important mechanism used for the generation of proteomic diversity and the regulation of gene expression in eukaryotic organisms [1]. Alternative splicing is often found to be regulated in tissue-specific, developmental and hormone-responsive manners and has been well documented in human [2] and other model eukaryotic organisms including mouse [3], *Drosophila* [4], *Arabidopsis* [5], and the free-living nematode *Caenorhabditis elegans* [6]. In contrast, examples of AS are only scarcely reported in the parasitic nematodes. The *fur* gene of *Dirofilaria immitis* [7] and the glutathione *S*-transferase 3 gene of *Onchocerca volvulus* [8] are among the few examples of alternatively spliced genes identified in animal-parasitic nematodes. However, studies on the functional consequences of AS are still lacking in this group of nematodes. In addition, no AS events have been identified in plant–parasitic nematodes.

Recently genes encoding chorismate mutase (CM), an enzyme previously found only in bacteria, fungi, and plants [9–11],

Abbreviations: AP, alkaline phosphatase; AS, alternative splicing; CM, chorismate mutase; DIG, digoxigenin; IPTG, isopropyl-β-D-thiogalactopyranoside; Mt-CM, *Mycobacterium tuberculosis* chorismate mutase; qRT-PCR, quantitative real-time reverse transcription-polymerase chain reaction; SNP, single nucleotide polymorphism; SP, signal peptide.

☆ *Note*: The nucleotide sequence data reported in this paper are available in the GenBank database under the accession numbers EF437152 (*Gr-cm-1A* genomic clone), EF437153 (*Gr-cm-1B* genomic clone), EF437154 (*Gr-cm-1* cDNA), EF437155 (*Gr-cm-1-IRII* cDNA), and EF437156 (*Gr-act-1* genomic clone).

* Corresponding author at: USDA-ARS, Robert W. Holley Center for Agriculture and Health, Ithaca, NY 14853, USA. Tel.: +1 607 255 3518; fax: +1 607 255 1132.
E-mail address: xw57@cornell.edu (X. Wang).
[1] Present address: Netafirm, Beijing, PR China.

0166-6851/$ – see front matter © 2008 Elsevier B.V. All rights reserved.
doi:10.1016/j.molbiopara.2008.06.002

have been cloned from several plant–parasitic nematode species [12–17]. Chorismate mutase is an important enzyme in the shikimate pathway that catalyzes the conversion of chorismate to prephenate [18]. In plants, the shikimate pathway not only produces precursors of phenylalanine, tyrosine, and tryptophan, but also precursors for a variety of aromatic secondary metabolites derived from chorismate [9,10,19]. These chorismate-derived compounds (CDCs), including indole-3-acetic acid (IAA), salicylic acid (SA), flavonoids, phytoalexins, and lignins, have diverse functions in plant growth, defence responses and interactions with other organisms [19].

All of the plant–parasitic nematode *CM* genes have been found to be expressed exclusively within the nematode's oesophageal gland cells and encode proteins with predicted N-terminal signal peptides [12–17]. The presence of signal peptides in the deduced proteins of phytonematode *CM* genes and their expression in the oesophageal gland cells indicate that they can be secreted into host roots. Studies have revealed that sedentary plant–parasitic nematodes (*Meloidogyne* spp. and *Heterodera* and *Globodera* spp.) secrete through their stylets a variety of proteins produced in their oesophageal gland cells and these secretory proteins play critical roles in nematode root invasion, the establishment and maintenance of nematode-induced feeding cells, and potential suppression of host defence responses [20–22]. The enzymatic activity of nematode CMs was confirmed by bacterial complementation [12,15] and biochemical assays [13]. Interestingly, overexpression of the *CM* gene from the root-knot nematode *Meloidogyne javanica* in soybean hairy roots produced a phenotype of reduced and aborted lateral roots and the altered root phenotype was found to be rescued by the exogenous application of IAA [23]. Doyle and Lambert [23] proposed that CM secreted by nematodes could alter plant cellular production and partitioning of specific CDCs to affect root cell development. A recent study demonstrated that RNAi silencing of the *CM* gene from the soybean cyst nematode *Heterodera glycines* resulted in altered sexual fate favoring male development on host roots, providing further evidence that nematode-secreted CM may contribute to successful parasitic interactions that favor egg-laying female development [24]. No *CM* gene homologues have been identified in *C. elegans* or animal parasitic nematodes, suggesting that the *CM* genes of plant–parasitic nematodes may have evolved unique functions in the parasitic interactions with host plants.

Potato cyst nematodes, *Globodera rostochiensis* and *Globodera pallida*, cause serious problems in potato production worldwide [25]. In spite of having a limited distribution in North America [25], these pests were recently detected in new locations in the U.S. [26] and Canada [27]. Because of the wide distribution and potential activity of *CM* homologues in phytonematodes, including *G. pallida* [14], we assayed *CM* homologues in *G. rostochiensis*. In this paper, we report the isolation and characterization of a new nematode *CM* gene from *G. rostochiensis*. Most importantly, we discovered that the pre-mRNA of the *G. rostochiensis CM* gene was subjected to alternative splicing through intron retention leading to two different mature mRNAs (*Gr-cm-1* and *Gr-cm-1-IRII*) that were revealed to have different expression profiles during nematode development. When translated, the alternatively spliced variant *Gr-cm-1-IRII* would result in a truncated protein (GR-CM-1t) lacking the CM domain. We used low-temperature SDS-PAGE analysis to reveal a potential dimeric structure of the CM protein (GR-CM-1) encoded by *Gr-cm-1*. Yeast two-hybrid analysis further demonstrated the specific interaction between GR-CM-1 and GR-CM-1t. This study provides the first identified example of AS in phytonematodes. A possible role of AS in regulating *G. rostochiensis* CM activity during plant parasitism is discussed.

2. Materials and methods

2.1. Nematode culture and inoculation

G. rostochiensis (pathotype Ro1) was propagated on greenhouse-grown susceptible potato (*Solanum tuberosum* cv. Katahdin) [28] and cysts were extracted as described previously [29]. Cysts were soaked in distilled water for 7 days and crushed to release the eggs. Preparasitic second-stage juveniles (pre-J2s) were collected by hatching eggs in potato root diffusate [30]. Collected pre-J2s were used for inoculation on monoxenic potato root cultures, nucleic acid extraction, *in situ* mRNA hybridization, and nematode genotyping experiments. Infected potato root materials that contained nematodes at different developmental stages were used as parasitic nematode materials for detecting *CM* gene expression using the quantitative real-time reverse transcription-PCR (qRT-PCR) assay described below. To obtain nematode-infected potato roots, true potato seeds of susceptible potato (*S. tuberosum*) were used for the generation of monoxenic root cultures in Petri dishes. The root cultures were grown at 24 °C on 1× MS agar medium (Sigma–Aldrich, St. Louis, MO) containing 1% sucrose. Freshly hatched pre-J2s were surface sterilized with 0.004% mercuric chloride, 0.004% sodium azide, and 0.002% Triton X-100 for 9 min, and rinsed several times with sterile distilled water. Surface-sterilized pre-J2s were resuspended in 0.1% low-melting agarose at a concentration of approximately 100 J2/10 μl. Five-microliter aliquots of pre-J2s were used to inoculate each root tip of potato grown monoxenically. Penetration of roots by pre-J2s was monitored using a dissecting microscope. Two days after nematode inoculation, excess pre-J2s were washed off from the plates to achieve a synchronized infection. Root segments that contained nematodes were collected at 2, 7, 10, 15, and 21 days post-inoculation (dpi) and transferred immediately to a −80 °C freezer. Roots collected at 2 and 7dpi were found to contain nematodes mainly at the parasitic J2 stage. Roots collected at 10, 15, and 21 dpi contained nematodes mostly at parasitic J3, J4, and young female stages, respectively. Uninfected roots were also collected and used as a negative control.

2.2. mRNA isolation and gene cloning

Frozen packed rehydrated cysts (~150), pre-J2s (~20,000–50,000), and infected potato root segments (containing 100–200 of parasitic stages of the nematode) were transferred respectively into a 2.0 ml Lysing Matrix D tube containing 1.4 mm ceramic spheres (QBiogene, Morgan Irvine, CA) and homogenized while the material was frozen using a Mini-Beadbeater-8 Cell Disrupter (BioSpec Products, Bartlesville, OK). The homogenized material was suspended in 1.0 ml of cold lysis/binding buffer (100 mM Tris–HCl, pH 7.5, 500 mM LiCl, 10 mM EDTA, pH 8.0, 1% LiDS, and 5 mM dithiothreitol) and mixed completely. Supernatant of the resulting suspension was collected after centrifugation and incubated with 1 mg of oligo$(dT)_{25}$ Dynabeads for mRNA extraction using the Dynabeads mRNA DIRECT Kit (Invitrogen, Carlsbad, CA) following the manufacturer's instructions. Bead-bound mRNA was finally eluted in 20–40 μl of 10 mM Tris–HCl, pH 8.0 and the concentration of mRNA obtained was determined using a BioSpec-mini Spectrophotometer (Shimadzu Corporation, Kyoto, Japan). 30-50 ng of mRNA was used for first-strand cDNA synthesis using the 3'RACE system (Invitrogen) according to the manufacturer's instructions. GpCM1F primer (Table 1) specific to the 5′-end of the *Gp-cm-1* gene (GenBank accession number AJ457834) of *G. pallida* [14] and degenerate CM1-R2 primer (Table 1) were used to amplify a partial *CM* cDNA from *G. rostochiensis* by PCR using first-stand cDNA obtained from pre-J2s as template. The CM1-R2 primer was designed according to the conserved internal sequence identified among *Gp-cm-1*

Table 1
Primers and probes used in this study

Name	Sequences (5′ → 3′)
Primers	
GpCM1F	GGTTTAATTACCCAAGTTTGAG
CM1-R2	TAGCRTYYATTTGGTCTTGGAA
CM1-ATGF	ATGAATTTGTTGGTCGTTCCGT
CM1-3endR	GTCAGGTTTTTACTTCATCTAATCTC
CM1-G1863F	CCAAGAAACTGCTGAATGAAT
CM1-G1936F	GCCCTATGTGTGGAGATTAGAT
CM1-G20R	GGAACGACCAACAAATTCAT
CM1-G136R	TACGATCAGTGCAATGCTTT
CM1A-G600F	CCCGCACACGCTGCCGGTAAATTT*
CM1B-G574F	TTCGCACAGTGAGGGCCGGACAC*
CM1-G1490R	GGTTTCACGGTACGCCTCACTAT
CM1-F2	CGGAATCGACAACGGGAAAT
CM1-569R	CGATGTTCCACATCTTCACGT
CM1t-335F	TCAAGGTACGGTCACTAAAT
CM1t-413R	CTGGTCAAAATGGTTACA
CM1-c302F	AGCCGAATCAAGAGACGGC**
CM1-1005FC	CGTCTGTAACCATTTTGACCA
CM1-c547Rb	CACGTAGCCCTTCTGAATG**
GrActin-c660Fb	CGACTTCGAGCAGGAAAT**
GrActin-R2b	ATGTCGATGTCGCACTTC
CM1-58F	*CACC*ATGGCAAAATCGCCCGCTCGT
CM1-861R	CTATTCATTCAGCAGTTTCTTGGC
CM1-858R	TTCATTCAGCAGTTTCTTGGCCT
CM1t-429R-HA	tcagccggcataatcaggtacatcataagggtaGGATCCGCCGTTTGTTGG CCATGCC
CM1-58F-E	*CCGGAATTC*CGCAAAATCGCCCGCTCGT
CM1-858R-B	*CGCGGATCC*TCATTCATTCAGCAGTTTCTTGGCCT
CM1t-429R-B	*CGCGGATCC*TCAGCCGTTTGTTGGCCATGCC
Probes	
CM1-c339F	FAM-CATGGCCAACAAACGGCTGATGT-TAMRA
GrActin-c808F	FAM-CCTCTTCCAGCCGTCCTTCATC-TAMRA**

Allele-specific primers are indicated by asterisk. Primers and probes that were designed to exon–exon boundaries are indicated by double asterisks and sequences corresponding to the upstream exon are underlined. Nucleotides incorporated in the 5′-ends of primers for cloning purpose are indicated in italics. The HA epitope sequence incorporated in the 5′ end of the CM1t-429R-HA primer is indicated in lower case.

(nucleotide positions 543–564), the *M. javanica CM* gene (*MjCM-1*, AF095949, positions 322–343) [12], and *M. incognita CM* genes (*Mi-cm-1*, AY422834, positions 322–343; *Mi-cm-2*, AY422835, positions 322–343) [15]. The partial *CM* cDNA was cloned and sequenced at the Cornell University DNA Sequencing Facility. Then the CM1-ATGF primer (Table 1 and Fig. 1) was designed and used with the abridged universal amplification primer (AUAP, Invitrogen) to obtain full-length cDNA of the *CM* gene (designated as *Gr-cm-1*) by PCR using first-strand cDNA from pre-J2s as template. The PCR cycling conditions were 94 °C for 1 min, followed by 30 cycles of 94 °C for 1 min, 55 °C for 1 min, 72 °C for 2 min, and a final reaction of 72 °C for 10 min. PCR-amplified products were cloned into the pCRII-TOPO vector (Invitrogen) and sequenced at the Cornell University DNA Sequencing Facility.

2.3. Genomic DNA extraction, genomic clones of Gr-cm-1, and Southern blot analysis

Packed pre-J2s (~100 μl) were resuspended in 0.5 ml of lysis solution (100 mM NaCl, 100 mM Tris–HCl, pH 8.0, 50 mM EDTA, pH 8.0, 1% SDS, 1% β-mercaptoethanol, and 100 μg/ml proteinase K, Invitrogen) and incubated at 65 °C for 30 min. Nematode DNA was extracted from the lysed mixture by phenol, phenol/chloroform (1:1), and chloroform extractions, then precipitated with 0.1 volume of 3 M sodium acetate (pH 5.5) and two volumes of absolute ethanol. Genomic DNA was finally resuspended in TE buffer (10 mM Tris–HCl, pH 7.5, and 1 mM EDTA). Plant genomic DNA was extracted from potato roots by grinding root tissues (~1.0 g) in a mortar containing 2 ml of extraction buffer (200 mM Tris–HCl, pH 8.0, 25 mM EDTA, pH 8.0, 250 mM NaCl, and 0.5% SDS), then by phenol/chloroform extraction and ethanol precipitation as described by Edwards et al. [31].

Gene-specific primers CM1-ATGF and CM1-3endR (Table 1 and Fig. 1), designed respectively to the 5′-end of the coding region (including the start codon ATG) and the 3′-end of the untranslated region of the *Gr-cm-1* cDNA, were used to amplify the corresponding genomic sequence from *G. rostochiensis* genomic DNA. The amplified PCR products were purified using the QIAquick Gel Extraction Kit (Qiagen, Valencia, CA) and cloned into the pCRII-TOPO vector (Invitrogen) for sequencing. To examine if *Gr-cm-1* is repeated in the nematode genome, PCR amplifications using different combinations of primers of CM1-G1863F, CM1-G1936F, CM1-G20R, and CM1-G136R (Table 1 and Fig. 1) and the *G. rostochiensis* genomic DNA (100 ng) were conducted. The PCR cycling conditions were 94 °C for 1 min, followed by 30 cycles of 94 °C for 1 min, 55 °C for 1 min, 68 °C for 10 min, and a final reaction of 72 °C for 10 min. Platinum *Taq* DNA Polymerase High Fidelity (Invitrogen) was used in PCR amplifications to ensure the ability of amplifying large DNA fragments.

Approximately 10 μg of nematode or plant genomic DNA was completely digested with *EcoRI, ClaI, HindIII* or *DraI*, separated by electrophoresis on a 0.7% agarose gel, transferred onto a positively charged nylon membrane (Roche Applied Science, Indianapolis, IN), fixed using a Spectrolinker XL-1000 UV crosslinker (Spectronics Corporation, Westbury, NY), and hybridized following a standard protocol [32]. A digoxigenin (DIG)-labeled probe corresponding to the open reading frame of the *Gr-cm-1* cDNA was generated by PCR with primers of CM1-ATGF and CM1-3endR using the PCR DIG Probe Synthesis Kit (Roche Applied Science). About 10 ng of DIG-labeled probe per ml was used for hybridization. Hybridization was performed at 65 °C for 14 h followed by two washes in 2× SSC/0.1% SDS at 65 °C for 30 min. After incubating the membrane in 1% blocking solution for 30 min, the membrane was incubated with a 1:5000 dilution of alkaline phosphatase (AP)-conjugated anti-DIG antibody (Roche Applied Science) for 30 min. Unbound antibody was removed by two 15 min washes with maleic acid washing buffer (Roche Applied Science). The membrane was finally washed in AP detection buffer (Roche Applied Science) and incubated with the chemiluminescent substrate CSPD (disodium 3-(4-methoxyspiro{1,2-dioxetane-3,2′-(5′-chloro)tricyclo[3.3.1.1^{3,7}]decan}-4-yl)pheryl phosphate) (Roche Applied Science) at 37 °C for 10 min followed by 2 h at room temperature in the dark. Signals were detected by exposing the membrane to Kodak X-OMAT X-ray film (Kodak, Rochester, NY) for 5–15 min.

2.4. Genotyping of individual pre-J2s

Genomic DNA from individual pre-J2s was prepared by incubating a single pre-J2 (manually picked under a microscope) in 5 μl of lysis buffer (40 mM Tris–HCl, pH 8.4, 100 mM KCl, and 0.5 μg/ml of proteinase K) at 65 °C for 1 h, followed by incubation at 95 °C for 15 min to inactivate proteinase K activity. Two microliters of the suspension was used for PCR analysis. A nested PCR assay was performed to detect the presence of *Gr-cm-1A* or *Gr-cm-1B* in individual pre-J2s. In the first PCR, primers CM1-ATGF and CM1-3endR were used to amplify both *Gr-cm-1A* and *Gr-cm-1B*. PCR was performed in a 25 μl reaction containing 12.5 μl of PCR Master Mix (Promega, Madison, WI), 1 μM of each primer, and 2 μl of genomic DNA. The cycling conditions were 94 °C for 1 min, followed by 30 cycles of 94 °C for 30 s, 55 °C for 30 s, and 72 °C for 1 min. The obtained PCR product(s) was 1:100 diluted and used as template for a second PCR amplification. Two separate reactions (A and B) were performed. *Gr-*

cm-1A-specific forward primer CM1A-G600F and the CM1-G1490R primer (Table 1 and Fig. 1) were used for the specific amplification of *Gr-cm-1A* (reaction A). *Gr-cm-1B*-specific forward primer CM1B-G574F (Table 1 and Fig. 1) and the CM1-G1490R primer were used for the specific amplification of *Gr-cm-1B* (reaction B). The specificity of these two primer pairs was confirmed by using corresponding genomic DNA clones as PCR templates and by sequencing confirmation of the amplified PCR products. The cycling conditions were the same as that of the first PCR. Final PCR products were checked on agarose gel by electrophoresis. If only reaction A produced an expected size of DNA product (951 bp), then the pre-J2 was genotyped as homozygous *Gr-cm-1A/A* (Table 2). If only reaction B produced an expected size of DNA product (917 bp), then the pre-J2 was genotyped as homozygous *Gr-cm-1B/B* (Table 2). The pre-J2 was genotyped as heterozygous *Gr-cm-1A/B* (Table 2) if both reactions produced DNA products of expected sizes. Some PCR products were purified and sequenced to confirm sequence identity.

2.5. In situ mRNA hybridization within nematode specimens

CM1-F2 and CM1-569R primers (Table 1) were used to synthesize DIG-labeled sense and antisense cDNA probes of the *Gr-cm-1* gene using the PCR DIG Probe Synthesis Kit (Roche Applied Science) by asymmetric PCR [33]. DIG-labeled sense and antisense cDNA probes targeting the 74-bp retained intron 2 identified in *Gr-cm-1-IRII* were also synthesized using primers CM1t-355F and CM1t-413R (Table 1) and this antisense probe should specifically recognize the *Gr-cm-1-IRII* transcript. Freshly hatched pre-J2s were fixed, permeabilized and used for *in situ* mRNA hybridization as described previously [33,34]. cDNA probes that hybridized within nematode specimens were detected by AP-conjugated anti-DIG antibody, BCIP-NBT substrate staining, and compound light microscope observation.

2.6. Developmental expression of Gr-cm-1 and Gr-cm-1-IRII

Quantitative real-time reverse transcription-PCR (qRT-PCR) was used to quantify the expression of *Gr-cm-1* and *Gr-cm-1-IRII* in nematode developmental stages. CM1-c339F probe (Table 1) hybridized specifically to both *Gr-cm-1* and *Gr-cm-1-IRII* and GrActin-c808F probe (Table 1) hybridized specifically to the *G. rostochiensis* β-actin gene (*Gr-act-1*, EF437156) were synthesized that contained a fluorescence reporter dye (6-carboxyfluorescein or FAM) and a quencher dye (6-carboxytetramethylrhodamine or TAMRA) at their 5′- and 3′-ends, respectively (Integrated DNA Technology, Coralville, IA). Primers CM1-c302F and CM1-c547Rb (Table 1 and Fig. 1) and probe CM1-c339F were used for the specific detection of the *Gr-cm-1* transcript. Primers CM1-1005FC and CM1-c547Rb (Table 1 and Fig. 1) and probe CM1-c339F were used for the specific detection of the *Gr-cm-1-IRII* transcript. Primers GrActin-c660Fb and GrActin-R2b (Table 1) and probe GrActin-c808F were used for the specific detection of the *Gr-act-1* transcript. *Gr-act-1* was used as an internal control for all of the cDNA samples tested. Primers CM1-c302F and CM1-c547Rb, and primer GrActin-c660Fb and probe GrActin-c808F were designed to span exon–exon junctions of the processed transcripts of *Gr-cm-1* and *Gr-act-1*, respectively, to prevent amplification/hybridization of any possible contaminating genomic DNA in the sample. The specificity of each primer/probe pair was confirmed using corresponding cDNA and genomic DNA clones as well as cDNA and genomic DNA obtained from uninfected plant roots as PCR templates.

qRT-PCR was carried out in an iCycler iQ Real-Time PCR Detection System (Bio-Rad Laboratories, Hercules, CA). The assay was conducted in a 96-well plate in a 25 μl reaction volume containing iQ Supermix (50 mM KCl, 20 mM Tris–HCl, pH 8.4, 0.8 mM dNTPs, 0.375 U iTaq DNA polymerase, 3 mM $MgCl_2$, and stabilizers) (Bio-Rad), 500 nM of both forward and reverse primers, 500 nM probe, and 1 μl of cDNA transcribed from each mRNA sample. Messenger RNA samples for each developmental stage were prepared from two independent experiments. PCR was started with an iTaq DNA polymerase activation and DNA denaturation step (95 °C for 3 min), then followed by 40 cycles of 95 °C for 20 s and 60 °C for 40 s. All qRT-PCR assays consisted of three technical replicates. Standard curves for *Gr-cm-1*, *Gr-cm-1-IRII*, and *Gr-act-1* were constructed following a standard protocol (User Bulletin 2, ABI PRISM 7700 Sequence Detection System, Applied Biosystems, Foster City, CA). Data were analyzed using the iCycler iQ Real-Time PCR Detection System Software version 3.0a (Bio-Rad). The calculated copy numbers of *Gr-cm-1* and *Gr-cm-1-IRII* in each sample were further normalized to *Gr-act-1* and the normalized values were plotted to indicate gene expression levels.

2.7. CM complementation

The *Gr-cm-1* coding region minus the putative signal peptide (SP) sequence was amplified by PCR from a *Gr-cm-1* cDNA clone with primers CM1-58F and CM1-861R (Table 1). The corresponding region of *Gr-cm-1-IRII* was amplified with CM1-58F and CM1-861R primers from a *Gr-cm-1-IRII* cDNA clone. The amplified PCR products were gel-purified and cloned into the pET101/D-TOPO vector (Invitrogen). The obtained recombinant constructs were sequenced to verify the sequence accuracy of the inserts and transformed into the CM-deficient *Escherichia coli* strain JP2261 (*aroF363, pheO352, pheA365*, *tryA382*, *thi-1*, *lac*, *tsx-358*, *rpsL712*, *xyl*) [35]. The obtained transformants were further analyzed by PCR to confirm the presence of the recombinant constructs. Transformed *E. coli* cells were grown in 5 ml of liquid M9 minimal medium supplemented with 100 μg/ml ampicillin, 0.3% glucose, 30 mg/l tyrosine, and 0.5 mg/l thiamine at 37 °C overnight with shaking and incubated for additional 3 h after addition of isopropyl-β-D-thiogalactopyranoside (IPTG) at a final concentration of 1 mM. The induced cells were spun down and resuspended in sterile distilled water at a concentration of OD_{600} = 0.3. Ten microliters of each cell suspension were dropped onto M9 minimal agar medium containing 100 μg/ml ampicillin, 0.3% glucose, 30 mg/l tyrosine, and 0.5 mg/l thiamine or LB-ampicillin agar medium and incubated at 37 °C for 24 h. The JP2261 strain containing only the pET101/D-TOPO vector was used as a negative control.

2.8. Expression in E. coli and Western blot analysis

The *Gr-cm-1* coding region (minus the putative SP) was amplified by PCR with primers CM1-58F and CM1-858R (Table 1) and cloned in frame with the V5 epitope tag of pET101 (Invitrogen). The V5-tagged GR-CM-1 protein is predicted to be 33.8 kDa and its expression can be induced by IPTG under the control of the T7*lac* promoter. The *Gr-cm-1-IRII* coding region (minus the putative SP) was amplified by PCR with primers CM1-58F and CM1t-429R-HA (Table 1) and cloned into pBAD202 (Invitrogen). The N-terminus of *Gr-cm-1-IRII* was cloned in frame with the thioredoxin domain of pBAD202 and the C-terminus of *Gr-cm-1-IRII* was incorporated an HA epitope derived from primer CM1t-429R-HA. The HA-tagged GR-CM-1t protein is predicted to be 29.0 kDa and its expression can be induced by arabinose under the control of the *ara*BAD promoter. These expression constructs were transformed individually or cotransformed into *E. coli* strain BL21 (Invitrogen) and the resulting transformants were selected for either a single or double antibiotic resistance. To obtain soluble expressed proteins, *E. coli* cultures were grown to a high density (OD_{600} = 2.0–2.5)

then IPTG (0.5–1 mM) and arabinose (0.02%) were added individually or together to respective cell cultures. The induced cultures were grown at low temperatures (30–35 °C) for 3 h before harvesting.

Collected *E. coli* cells were lysed using the BugBuster protein extraction reagent (EMD, San Diego, CA) according to the manufacturer's instructions. Soluble proteins were collected and protein concentrations were determined. Low-temperature SDS-PAGE [36,37] was performed to detect the formation of homodimers of GR-CM-1 and potential heterodimers formed between GR-CM-1 and GR-CM-1t. Extracted soluble proteins (approximately 15 μg per lane) were incubated at 95 °C for 5 min for denaturation or at 37 °C for 10 min followed by 30 min on ice for preservation of dimerization, and then were subjected to SDS-PAGE and subsequently transferred onto a PVDF membrane (Invitrogen). After blocking, the membrane was incubated with the anti-V5 AP conjugated antibody (1:5000 dilution) (Invitrogen) for detection of the V5-tagged GR-CM-1 protein or the anti-HA horseradish peroxidase (HRP) conjugated antibody (1:10,000 dilution) (Roche Applied Science) for detection of the HA-tagged GR-CM-1t protein. In order to detect proteins on the same blot with different antibodies, the membrane was first incubated with the anti-V5 antibody, then stripped off of the bound anti-V5 antibody by incubation in the stripping solution (25 mM glycine–HCl, pH 2.0, and 1% SDS) for 30 min followed by washing twice in PBS buffer for 10 min. The membrane was subsequently incubated with the anti-HA antibody. Bands were visualized by using the Immobilon Western Chemiluminescent AP or HRP substrate (Millipore, Billerica, MA) following exposure to Kodak X-OMAT X-ray films (Kodak).

2.9. Yeast two-hybrid analysis

The MATCHMAKER two-hybrid system 3 (Clontech, Mountain View, CA) was used to test a potential interaction between GR-CM-1 and GR-CM-1t. *Gr-cm-1* and *Gr-cm-1-IRII* coding regions (minus the putative SP) were amplified by PCR with primer pairs of CM1-58F-E and CM1-858R-B and CM1-58F-E and CM1t-429R-B, and cloned in frame with the GAL4 activation domain (AD) of the prey vector pGADT7 and the GAL4 DNA-binding domain (BD) of the bait vector pGBKT7, respectively. The resulting constructs pGBKT7–*Gr-cm-1t* and pGADT7–*Gr-cm-1* were cotransformed into strain AH109. To exclude a possibility of autoactivation, AH109 strains cotransformed with pGBKT7–*Gr-cm-1t* and pGADT7-*RecT* (Clotech) or pGBKT7-*Lam* (Clotech) and pGADT7–*Gr-cm-1* were included in the assays. In addition, AH109 strains cotransformed with pGBKT7-*53* (Clotech) and pGADT7-*RecT* or pGBKT7-*Lam* and pGADT7-*RecT* were used as positive and negative controls. All procedures including yeast transformation, selection of positive clones, and the assay of β-galactosidase activity were conducted following the manufacturer's instructions.

2.10. Phylogenetic and computer analyses

BLASTP searches against the GenBank databases at the NCBI website (http://www.ncbi.nlm.nih.gov/BLAST/) [38] were performed to identify GR-CM-1 protein homologues, and the Conserved Domain Search (CD-Search) program [39] was used to examine the presence of a conserved CM domain in the identified homologues. Signal peptide analysis was conducted using the SignalP program [40]. For phylogenetic analysis, CM domains of GR-CM-1 protein homologues were aligned using the CLUSTAL X program [41]. The CM domains of plant and fungal CMs were found to be divergent from those of nematode and bacterial CMs, therefore, a manual adjustment based on structure similarity to the CM domains of *Mycobacterium tuberculosis* and *Saccharomyces cerevisiae* CMs [42] was made to ensure alignment accuracy. The CLUSTAL X alignment data was analyzed with the PHYLIP 3.61 package using the neighbor-joining method (http://evolution.genetics.washington.edu/phylip.html) [43]. The consensus tree (from 1000 bootstrap replicates) was drawn using the TreeView software (http://taxonomy.zoology.gla.ac.uk/rod/treeview.html).

3. Results

3.1. The G. rostochiensis chorismate mutase cDNAs

A series of primer pairs (data not shown), designed according to the *Gp-cm-1* gene (GenBank accession number AJ45834) of *G. pallida* and the conserved regions among *Gp-cm-1*, the *M. javanica CM* gene (*MjCM-1*, AF095949) [12], and *M. incognita CM* genes (*Mi-cm-1*, AY422834; *Mi-cm-2*, AY422835) [15], were used to isolate *CM* gene homologues in *G. rostochiensis*. Only primer GpCM1F (Table 1) corresponding to the spliced leader SL1 sequence of *Gp-cm-1* and an internal degenerate primer CM1-R2 (Table 1) produced a PCR product from transcripts of preparasitic second-stage juveniles (pre-J2s) of *G. rostochiensis*. Initial sequence analysis identified two partial cDNA clones that were revealed to have significant similarity to *CM* genes from phytonematodes. The full-length sequences of the two *CM* cDNAs (designated as *Gr-cm-1* and *Gr-cm-1-IRII*) (Fig. 1) were further obtained using a 3′ RACE system and found to be 992 bp (*Gr-cm-1*, EF437154) and 1069 bp (*Gr-cm-1-IRII*, EF437155) long, respectively. The *Gr-cm-1* cDNA contained an open reading frame (ORF) of 861 bp (Fig. 1) that encoded a predicted protein of 286 amino acids. The deduced GR-CM-1 protein was predicted by the SignalP program [40] to contain a N-terminal signal peptide, resulting in a mature GR-CM-1 protein with an estimated molecular weight of 30,106 Da. At the amino acid level, the GR-CM-1 protein was 89.2% identical to the *G. pallida* CM, 53.7% identical to the *H. glycines* CM (encoded by *Hg-cm-1*, AY160225) [13], 52% identical to the *H. schachtii* CM (encoded by *Hs-cm-1*, DQ176596), 24.6% identical to the *M. javanica* CM, 23% and 22.5% identical to the *M. incognita* CM 1 and 2, respectively, and only 17% identical to the CM domain of *E. coli* CM [44]. The *Gr-cm-1-IRII* cDNA was identical to *Gr-cm-1* in the area of sequence overlap, but a 74-bp fragment was found to be inserted in the internal region of *Gr-cm-1-IRII* (Fig. 1). The *Gr-cm-1-IRII* cDNA contained an ORF of 432 bp (Fig. 1) that encoded a deduced truncated protein (GR-CM-1t) of 143 amino acids that lacked 182 amino acids of the C-terminal region of the GR-CM-1 protein but gained another 39 amino acids due to the generation of a stop codon caused by the insertion of the 74-bp fragment (Figs. 1 and 2).

3.2. Genomic clones and sequence analysis

The genomic sequences corresponding to *Gr-cm-1* and *Gr-cm-1-IRII* were obtained by PCR amplification from *G. rostochiensis* genomic DNA. Sequencing of more than 30 random clones from independent PCR reactions identified two different genomic sequences, and both of them matched to the *Gr-cm-1* cDNA except that three introns were found as indicated in Fig. 1. In these two genomic DNA clones, designated as *Gr-cm-1A* (EF437152) and *Gr-cm-1B* (EF437153), their three introns followed the 'GU-AG' rule for *cis*-splicing, but the 5′ splice site of intron 2 (AG/GTACGG) (Fig. 2) was unusual compared to the consensus 5′ splice site (AG/GTRAGT) identified in *C. elegans* [45]. *Gr-cm-1A* and *Gr-cm-1B* had identical intron 2 sequences and their intron 3 sequences were almost identical with only two dissimilar nucleotides that were

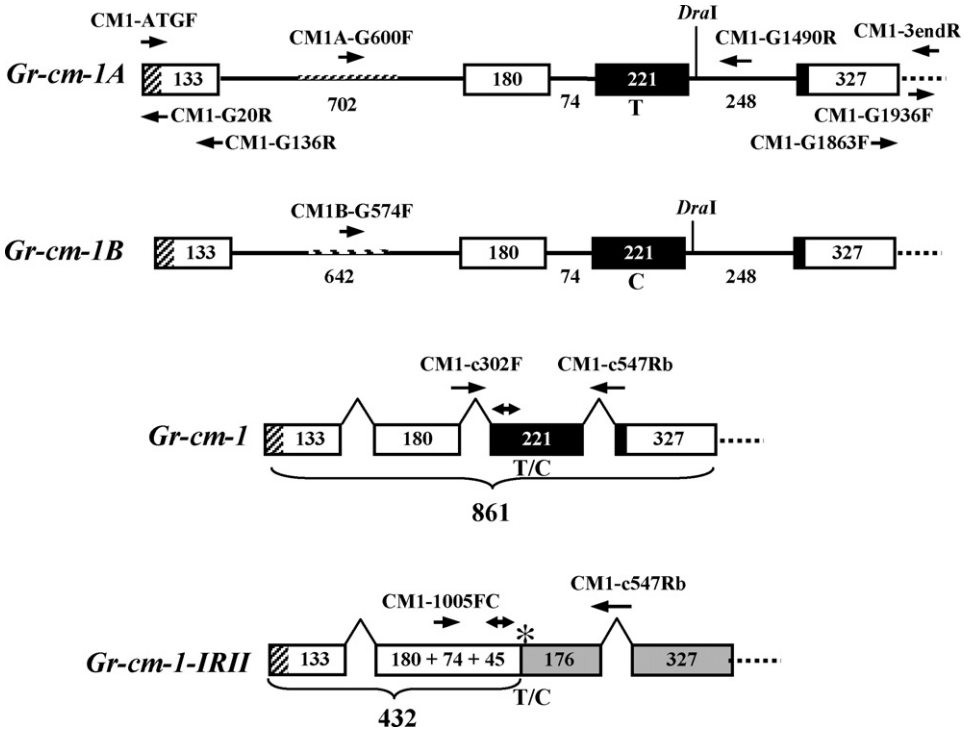

Fig. 1. Schematic diagrams of the genomic organization of *Gr-cm-1A* and *Gr-cm-1B* and the two mRNA transcripts of the *Gr-cm-1* gene. Exons are indicated by boxes (stippled boxes indicate the N-terminal signal peptide; black boxes indicate the chorismate mutase domain). Introns are indicated by solid lines (the stippled lines indicate the 200 bp dissimilar region between *Gr-cm-1A* and *Gr-cm-1B* in intron 1). The 3′-end untranslated region is indicated by dashed lines and the unique *DraI* digestion site is marked. Caret lines indicate exon–exon junctions in mRNA transcripts. Numbers in the boxes and below the lines indicate the sizes (in base pairs) of the exons and the introns, respectively. Numbers under the brackets indicate the sizes of the open reading frames of *Gr-cm-1* and *Gr-cm-1-IRII*, respectively. Primers (indicated by arrows), TaqMan probes (indicated by double arrows), and the synonymous single nucleotide polymorphism (SNP) (T in *Gr-cm-1A* vs. C in *Gr-cm-1B* in exon 3) are also schematically indicated. In *Gr-cm-1-IRII*, the alternative exon 2 also includes intron 2 (74 bp) and a region (45 bp) corresponding to the 5′-end of *Gr-cm-1* exon 3. The rest of the region in *Gr-cm-1-IRII* that corresponds to exons 3 and 4 of *Gr-cm-1* becomes noncoding exons (shaded) because of the presence of a premature stop codon (indicated by an asterisk).

confirmed to be unique for each sequence (Fig. 2). However, an obvious sequence variation was identified in the intron 1 regions of *Gr-cm-1A* and *Gr-cm-1B* that contained about 200 bp of very dissimilar sequences (Fig. 2). *Gr-cm-1A* and *Gr-cm-1B* contained four identical exons except for the third exon where a synonymous single nucleotide polymorphism (SNP) (T in *Gr-cm-1A* versus C in *Gr-cm-1B*) was identified (Figs. 1 and 2). Further sequence analysis revealed that the 74-bp insertion found in the *Gr-cm-1-IRII* cDNA was derived from the entire second intron of the genomic sequence, indicating that *Gr-cm-1-IRII* is a splice variant generated from the *Gr-cm-1* pre-mRNA by alternative splicing (AS). Additional sequencing of more than 50 cDNA clones revealed that more than half of the mRNA transcripts of the *Gr-cm-1* gene obtained from pre-J2s had intron 2 retained (data not shown). The presence of the intron-retained splice variant of the *Gr-cm-1* gene was further confirmed by a qRT-PCR assay as discussed below (in Section 3.4).

Table 2
Gr-cm-1 genotype in *G. rostochiensis* pathotype Ro1

Genotype			Allele frequency	
Gr-cm-1A/A	*Gr-cm-1B/B*	*Gr-cm-1A/B*	*A*	*B*
77/121 (63.6%)	5/121 (4.1%)	39/121 (32.3%)	79.8%	20.2%

Individual pre-J2s were randomly picked and genotyped using a nested PCR assay (in Section 2.4). The number of *G. rostochiensis* pre-J2s that were scored for each genotype is listed first, followed by the total number of individuals genotyped. The percentage of each genotype in the population is indicated in parenthesis. The allele frequencies are also listed in the table.

Gr-cm-1 genomic clones did not contain *EcoRI, ClaI* or *HindIII* restriction sites, but did contain one *DraI* digestion site (Fig. 1). Although two different genomic sequences of *Gr-cm-1* were identified, when DIG-labeled *Gr-cm-1* cDNA probe was hybridized to a membrane containing *EcoRI, ClaI, HindIII* or *DraI*-digested genomic DNA from *G. rostochiensis*, only one fragment was detected on the membrane with *EcoRI, ClaI* or *HindIII* digestion and two fragments were detected with *DraI* digestion (Fig. 3). To exclude the possibility of a repeated arrangement of *Gr-cm-1* in the genome, PCR amplifications designed to obtain potential intergenic region(s) between *Gr-cm-1* genes using one 3′ end forward primer of CM1-G1936F or CM1-G1863F (Table 1 and Fig. 1) and one 5′ end reverse primer of CM1-G20R or CM1-G136R (Table 1 and Fig. 1) or only a single primer of CM1-G1936F, CM1-G1863F, CM1-G20R, or CM1-G136R were conducted. However, none of the amplifications produced a PCR product (data not shown). Taken together, these results indicated that *Gr-cm-1* exists as a single-copy gene in the *G. rostochiensis* genome. No hybridization signal was detected with genomic DNA from *H. glycines* or potato (used as negative controls) (Fig. 3).

We hypothesized that *Gr-cm-1A* and *Gr-cm-1B* could represent different alleles of the *Gr-cm-1* gene in the nematode population. Therefore, individual pre-J2s were genotyped to test this hypothesis. When individual pre-J2s were genotyped with a nested PCR assay using allele-specific primers (Table 1) targeting the dissimilar intron 1 regions of *Gr-cm-1A* and *Gr-cm-1B* (Fig. 1), we found that in some individuals only *Gr-cm-1A* or *Gr-cm-1B* could be detected, whereas in others both *Gr-cm-1A* and *Gr-cm-1B* were detected. Since *G. rostochiensis* has a diploid genome and some of the pre-J2 individuals contained only one type of the *Gr-cm-1* genomic

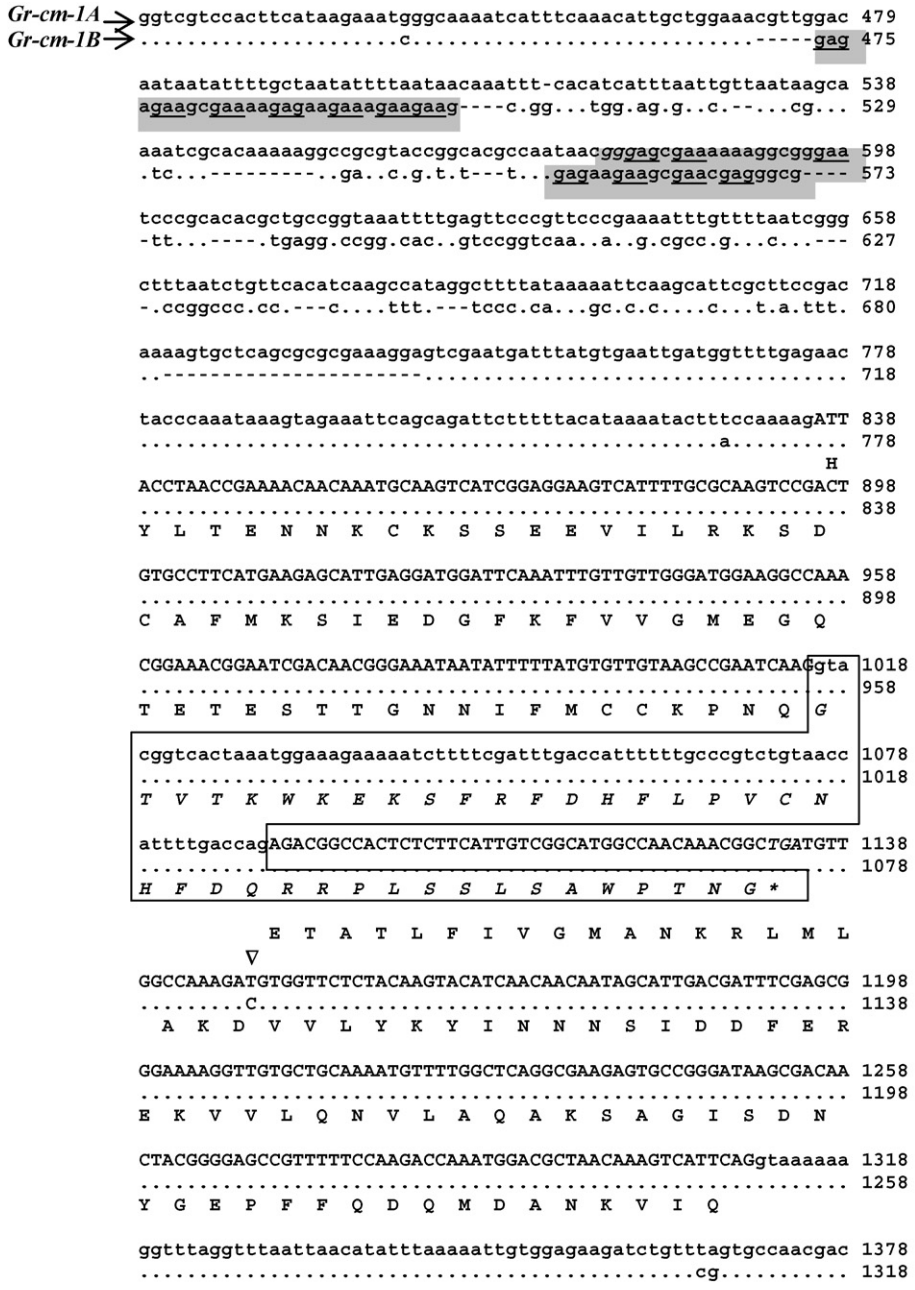

Fig. 2. Genomic sequences of *Gr-cm-1A* (top nucleotide sequence) and *Gr-cm-1B* (bottom nucleotide sequence) showing differences between the two alleles and the corresponding deduced amino acid sequences of *Gr-cm-1* and *Gr-cm-1-IRII*. Exon sequences are indicated in upper case. Intron sequences are indicated in lower case. Purine-rich elements are highlighted and the GAR (R = purine)-like repeats are underlined. The triangle indicates the synonymous SNP in exon 3. The intron 2 sequence is boxed and the newly derived amino acid sequence of *Gr-cm-1-IRII* caused by retention of intron 2 is indicated in italics with a stop codon marked as an asterisk. Deduced amino acid sequence of exons 2 and 3 of *Gr-cm-1* is shown below the corresponding nucleotide sequences.

sequences, we concluded that *Gr-cm-1A* and *Gr-cm-1B* represented different alleles of *Gr-cm-1*. The genotype of pre-J2 individuals can be homozygous (*Gr-cm-1A*/*A* or *Gr-cm-1B*/*B*) if only one type of the genomic sequences is detected, or heterozygous (*Gr-cm-1A*/*B*) if both types of the genomic sequences are detected (Table 2). In addition, our analysis revealed that 63.6% of the pre-J2s in the population were homozygous *Gr-cm-1A*/*A*, 4.1% were homozygous *Gr-cm-1B*/*B*, and 32.2% were heterozygous *Gr-cm-1A*/*B*. The allele frequencies were 79.8% for *Gr-cm-1A* and 20.2% for *Gr-cm-1B* (Table 2). A close examination of the intron 1 regions of *Gr-cm-1A* and *Gr-cm-1B* identified three short purine-rich stretches that contained repeats of the trinucleotide GAR (R = purine) and the G tracts (Fig. 2). These purine-rich stretches resembled the intronic splicing enhancers (ISEs) identified in the mammalian thyroid hormone receptor gene *c-erbAα* [46] and the human apolipoprotein A-II gene [47]. *Gr-cm-1A* contained only one purine-rich element, whereas *Gr-cm-1B* contained two such elements (Fig. 2). No purine-rich element was found in any other nematode *CM* genes (data not shown). As mentioned earlier, a SNP (T in *Gr-cm-1A* versus C in *Gr-cm-1B*) was also identified in exon 3. Sequencing of more than 50 random cDNA clones of the *Gr-cm-1* gene revealed that 86% of the intron-retained transcripts were originated from the

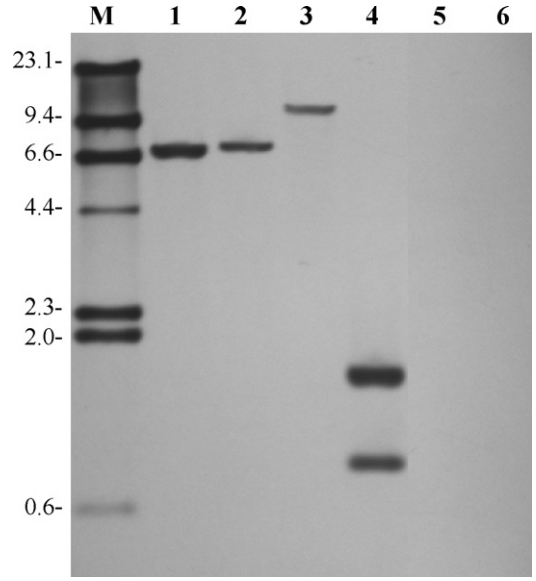

Fig. 3. Southern blot analysis of the *Gr-cm-1* gene. Genomic DNA from *Globodera rostochiensis* (lanes 1–4), *Heterodera glycines* (lane 5), and potato (lane 6) was digested with *EcoRI* (lane 1), *ClaI* (lane 2), *HindIII* (lanes 3, 5, and 6) or *DraI* (lane 4) and hybridized with the *Gr-cm-1* cDNA probe. M: DIG-labeled molecular weight marker in kilobases.

Gr-cm-1A allele (with T in the corresponding location) and only 14% were from the *Gr-cm-1B* allele (with C in the corresponding location). However, it is unclear if these putative *cis*-acting elements affect the splicing efficiency of intron 2 of the *Gr-cm-1* gene.

3.3. Similarity and phylogenetic relationship of GR-CM-1 to known chorismate mutases

BLASTP searches [38] revealed that the predicted GR-CM-1 protein was more similar to CMs from cyst nematodes and bacteria of the genus *Burkholderia* than to those from the root-knot nematodes. We further found that almost all of the bacterial CMs that had similarity to GR-CM-1 with a BLASTP E-value less than 0.001 contained predicted N-terminal signal peptides as found in nematode CMs. GR-CM-1 contained a predicted N-terminal signal peptide (SP) (residues 1–19) and a conserved CM domain (residues 111–179). Of the 11 active site amino acid residues identified in the *E. coli* CM [44], seven identical and three similar active site residues were found in the GR-CM-1 CM domain (Fig. 4). In addition, a long internal region (>70 aa) between the predicted SP and the CM domain was found only in GR-CM-1 and two other cyst nematode CMs (Fig. 4). However, the deduced truncated protein GR-CM-1t encoded by *Gr-cm-1-IRII* lacked the CM domain due to the presence of a premature stop codon because of retention of intron 2 (Figs. 1 and 2). Phylogenetic analysis using the conserved CM domains of CM proteins showed that nematode CMs were more closely related to the *AroQ bacterial periplasmic CMs than to the AroQ CMs from plant, fungi, and bacteria (Fig. 5). The AroQ class of CMs is widely distributed in both eukaryotes and prokaryotes in which a subclass denoted as *AroQ is described [48–50]. *AroQ CMs are secreted CMs with N-terminal signal peptides and may play a role in bacterial pathogenesis [42,51,52]. The *Mycobacterium tuberculosis* CM (Mt-CM) is the only CM from *AroQ CMs with a known crystal structure and determined to be an all-helical dimeric protein [42]. Our sequence alignment indicated that nematode CMs might have a similar protein folding structure as Mt-CM (Fig. 4). In addition, cyst and root-knot nematode CMs, except MA-CM-1 [16], were clustered into two separate groups based on our analysis (Fig. 5).

3.4. Spatial and developmental expression of Gr-cm-1 and Gr-cm-1-IRII

In situ mRNA hybridization was used to determine the spatial expression of *Gr-cm-1* in *G. rostochiensis*. The DIG-labeled antisense cDNA probe that could recognize both transcripts of *Gr-cm-1* and *Gr-cm-1-IRII* gave a hybridization signal specifically within the subventral oesophageal gland cells of both pre-J2s (Fig. 6A, left panel) and parasitic stages of the nematode (Fig. 6A, right panel). *Gr-cm-1* and *Gr-cm-1-IRII* are identical except for the retained intron 2 identified in *Gr-cm-1-IRII* (Fig. 1). The *Gr-cm-1-IRII*-specific antisense probe targeting the retained intron 2 region also detected a hybridization signal within the subventral gland cells of pre-J2s (Fig. 6A, middle panel), thus confirming the expression of the splice variant *Gr-cm-1-IRII* in the pre-J2 stage. This *Gr-cm-1-IRII*-specific probe only revealed a much weaker signal in parasitic stages (data not shown) compared to that in the pre-J2 stage. No hybridization signal was detected within the nematode specimens with the control sense cDNA probes (data not shown).

We further used qRT-PCR to examine the expression of *Gr-cm-1* and *Gr-cm-1-IRII* in different nematode developmental stages. Since the three cDNA-specific primer pairs (Table 1) designed specifically to *Gr-cm-1*, *Gr-cm-1-IRII*, and the internal control *Gr-act-1* did not amplify any product from cDNA obtained from uninfected potato roots (data not shown), infected roots that contained nematodes at different developmental stages were used as parasitic nematode materials for qRT-PCR analysis. Both *Gr-cm-1* and *Gr-cm-1-IRII* were revealed to be differentially expressed throughout the nematode life cycle. In the pre-J2 stage, *Gr-cm-1* and *Gr-cm-1-IRII* had comparable expression levels. However, in early parasitic stages, e.g., at 2, 7, and 10 days post-inoculation (dpi), the expression of *Gr-cm-1* was up-regulated (2- to 4-fold) whereas the expression of *Gr-cm-1-IRII* was down-regulated compared to those in the pre-J2 stage (Fig. 6B). In late parasitic stages (at 15 and 21 dpi), the expression of *Gr-cm-1* was maintained at a low level comparable to that in the pre-J2 stage but the expression of *Gr-cm-1-IRII* was further down-regulated (approximately 4-fold) (Fig. 6B). The magnitude of *Gr-cm-1-IRII* expression was only around 16% (at 7 dpi) to 29% of *Gr-cm-1* in the parasitic stages. The expression of both transcripts was low in the cyst stage (Fig. 6B).

3.5. Complementation assay for CM activity

Complementation of the CM-deficient *E. coli* strain JP2261 was used to determine if *Gr-cm-1* encodes a functional CM. Strain JP2261 lacks CM and prephenate dehydrogenase activities, therefore it cannot grow on minimal medium without supplemental phenylalanine and tyrosine [35]. JP2261 strains transformed with the pET101/D-TOPO expression vector or the construct carrying the *Gr-cm-1* cDNA (coding region minus the SP) or the *Gr-cm-1-IRII* cDNA grew normally on LB-ampicillin agar medium (Fig. 7A), but only the strain expressing the *Gr-cm-1* cDNA could grow on the minimal medium in the absence of phenylalanine (Fig. 7B), revealing that expression of GR-CM-1 could rescue the CM defect of JP2261. No rescue of the CM defect was observed with the other two transformed strains (Fig. 7B). These results suggested that *Gr-cm-1* encoded a functional CM and the CM domain of the GR-CM-1 protein was essential for protein function.

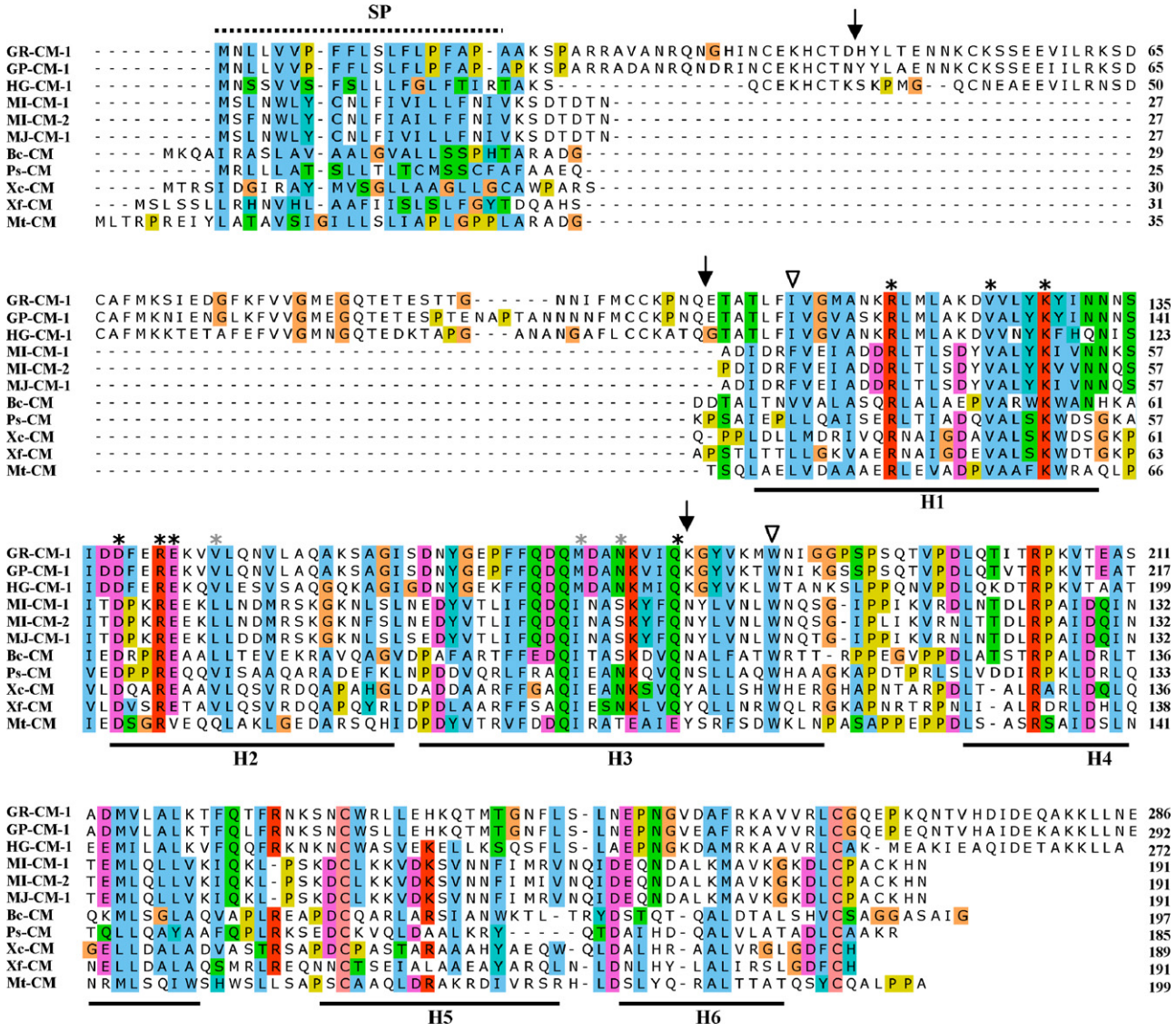

Fig. 4. Sequence alignment of *G. rostochiensis* chorismate mutase (CM) protein with secreted CMs from other plant–parasitic nematodes and pathogenic bacteria. Other secreted CM proteins include GP-CM-1 (accession number AJ457834) from *Globodera pallida*, HG-CM-1 (AY160225) from *Heterodera glycines*, MJ-CM-1 (AF095949) from *Meloidogyne javanica*, MI-CM-1 (AY422834) and MI-CM-2 (AY422835) from *M. incognita*, Bc-CM (ABI86426) from *Burkholderia cenocepacia* AMMD, Ps-CM (AAO53901) from *Pseudomonas syringae* pv. tomato str. DC3000, Xc-CM (CAJ25496) from *Xanthomonas campestris* pv. *vesicatoria*, Xf-CM (AAO28305) from *Xylella fastidiosa* str. Temecula1, and Mt-CM (NP_216401) from *Mycobacterium tuberculosis* H37Rv. The alignment was made using the CLUSTAL X program [41] in combination with a manual adjustment of the N-terminal signal peptide (SP) region (indicated by a dashed line) and the long internal region found only in cyst nematode CMs. Identical or similar amino acids are shaded and active site residues corresponding to those identified in *Escherichia coli* CM [44] are indicated by black (for identical residues) or grey (for similar residues) asterisks above the alignment. Conserved regions (H1-H6) corresponding to the six α-helices identified in Mt-CM [42] are indicated by black lines below the sequences. Vertical arrows indicate the positions of the three introns present in the genomic sequence of the *Gr-cm-1* gene. Triangles indicate borders of the most conserved CM domain.

3.6. Dimeric nature of GR-CM-1 and the specific interaction between GR-CM-1 and GR-CM-1t

Our phylogenetic analysis suggested that CMs from *G. rostochiensis* and other phytonematode species are closely related to the bacterial secreted *AroQ CMs that belong to a subgroup of the AroQ class of CMs. All characterized members of the AroQ family including the secreted Mt-CM share a dimeric structure [42,44,50,53–55]. We speculated that the full-length GR-CM-1 protein may have a structure and enzymatic property similar to the secreted Mt-CM. To examine a potential dimeric nature of GR-CM-1, we conducted low-temperature SDS-PAGE analysis [36,37]. GR-CM-1 was expressed as a V5-tagged protein in *E. coli*. As expected, both homodimers with an expected molecular weight of approximately 68 kDa and monomers of GR-CM-1 were detected by the anti-V5 antibody when the sample was treated under a non-denaturing condition (Fig. 8A, lane 1). No basal expression of GR-CM-1 was detected in the transformant (Fig. 8A, lanes 3 and 4). In an attempt to study the potential functional consequence of the alternatively spliced variant *Gr-cm-1-IRII*, V5-tagged GR-CM-1 expression construct and HA-tagged GR-CM-1t expression construct were cotransformed into *E. coli*. Expression of GR-CM-1 protein alone in the *E. coli* cotransformant could also produce both monomers and homodimers detectable by the anti-V5 antibody (Fig. 8B, lane 1, upper panel). Interestingly, both homodimers with an expected molecular weight of approximately 58 kDa and monomers of GR-CM-1t were also detected by the anti-HA antibody when the cotransformant was induced by a single inducer of arabinose (Fig. 8B, lane 3, lower panel). The formation of homodimers indicates that the dimerization domain is preserved in the

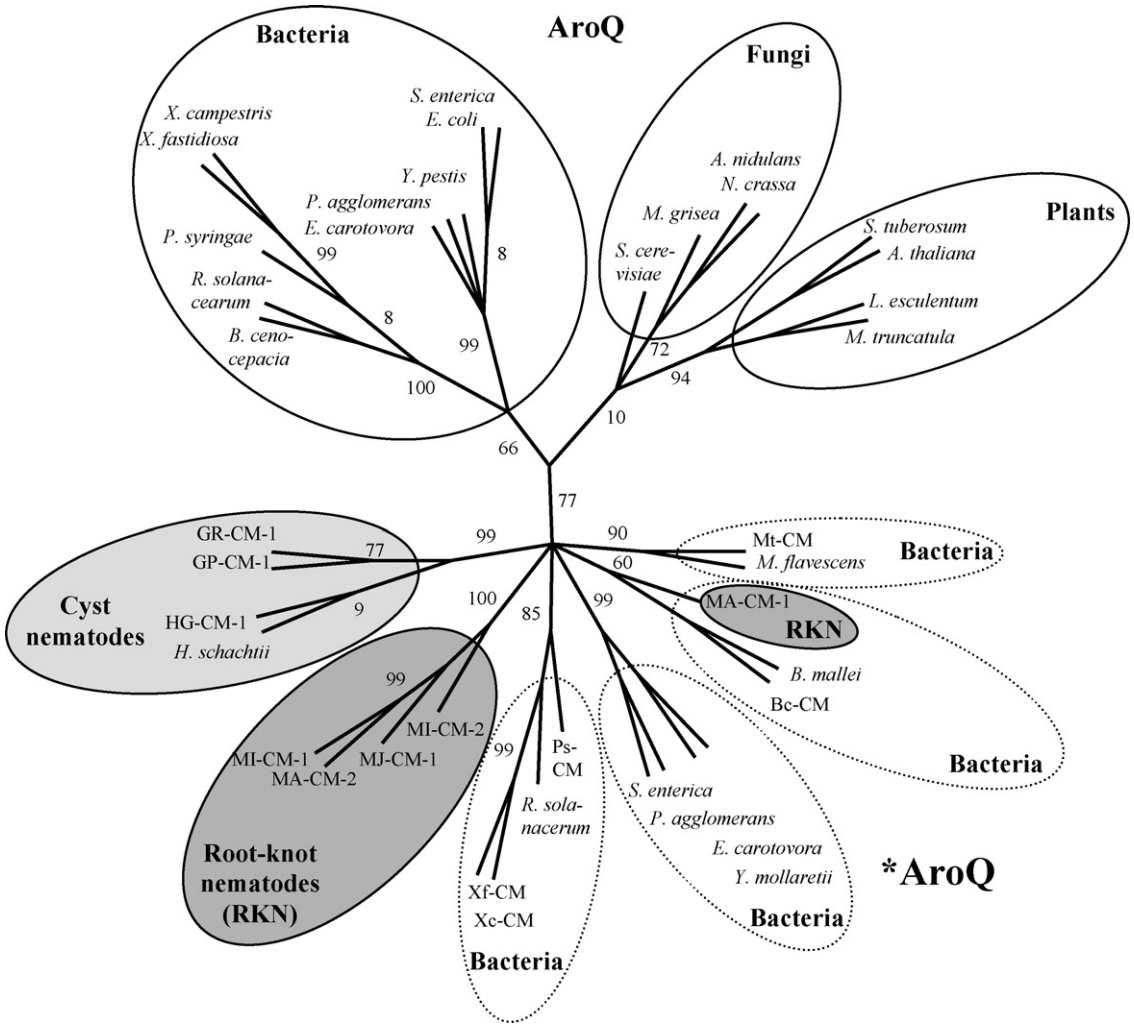

Fig. 5. Phylogenetic relationship of nematode CMs to CMs from plants, fungi and bacteria. Nematode CMs (shaded ovals) are found to be more closely related to the secreted *AroQ CMs of bacteria (dashed ovals) than to the AroQ CMs of bacteria, fungi, and plants (open ovals). Multiple sequence alignment was obtained using the CLUSTAL X program [41] and the unrooted consensus tree (from 1,000 bootstrap replicates) was generated using the PHYLIP 3.61 programs [43]. Analyzed secreted *AroQ CMs include GR-CM-1 (EF437154) from *G. rostochiensis*, GP-CM-1 (AJ457834) from *G. pallida*, HG-CM-1 (AY160225) from *Heterodera glycines*, Hs-CM-1 (DQ176596) from *H. schachtii*, MI-CM-1 (AY422834) and MI-CM-2 (AY422835) from *Meloidogyne incognita*, MJ-CM-1 (AF095949) from *M. javanica*, MA-CM-1 (DQ222223) and MA-CM-2 (DQ279096) from *M. arenaria*, Bc-CM (ABI86426) from *Burkholderia cenocepacia* AMMD, Ps-CM (AAO53901) from *Pseudomonas syringae* pv. tomato str. DC3000, Xc-CM (CAJ25496) from *Xanthomonas campestris* pv. *vesicatoria*, Xf-CM (AAO28305) from *Xylella fastidiosa* str. Temecula1, Mt-CM (NP_216401) from *Mycobacterium tuberculosis* H37Rv., and CMs from *Burkholderia mallei* ATCC 23344 (AAU49238), *Erwinia carotovora* subsp. *atroseptica* SCRI1043 (CAG74359), *Mycobacterium flavescens* PYR-GCK (ABP44155), *Pantoea agglomerans* ATCC 33243 (AAA73360), *Ralstonia solanacearum* GMI1000 (CAD17348), *Salmonella enterica* subsp. *enterica* (AAV77508), and *Yersinia mollaretii* ATCC 43969 (ZP_00826869). Analyzed AroQ CMs include CMs from *B. cenocepacia* AU 1054 (ABF75475), *E. carotovora* subsp. *atroseptica* (YP_051439), *Escherichia coli* (ZP_00735647), *P. agglomera* ATCC 33243 (AAA24853), *P. syringae* pv. tomato str. DC3000 (AAO55267), *R. solanacearum* GMI1000 (CAD14606), *S. enterica* subsp. *enterica* (AAX66575), *X. campestris* pv. campestris str. 8004 (AAY49693), *X. fastidiosa* str. Temecula1 (AAO29204), *Yersinia pestis* Nepal516 (ABG17147), *Aspergillus nidulans* (XP_664470), *Magnaporthe grisea* (XP_363784), *Neurospora crassa* (XP_961975), *Saccharomyces cerevisiae* (AAT93198), *Arabidopsis thaliana* (NP_566846), *Lycopersicon esculentum* (AAD48923), *Medicago truncatula* (ABE94587), and *Solanum tuberosum* (potato EST TC11504).

truncated GR-CM-1t protein. In addition, these results further confirmed that both V5-tagged GR-CM-1 and HA-tagged GR-CM-1t proteins could be individually expressed in the cotransformant under the control of their responsive promoters (Fig. 8B, lanes 1–4). When both tagged proteins were coexpressed in *E. coli* (Fig. 8B, lanes 5 and 6), interestingly however, only homodimers of GR-CM-1t along with monomers of GR-CM-1 and GR-CM-1t were detected (Fig. 8B, lane 5). GR-CM-1 was found to have a much lower expression level than GR-CM-1t, demonstrated in our Western blot analysis, which revealed that a much longer exposure time (at least five times longer) was needed to detect signals of GR-CM-1 with intensity similar to those of GR-CM-1t. It was unexpected that the formation of GR-CM-1 homodimers was undetectable (Fig. 8B, lane 5, upper panel); this may be due to the low expression of GR-CM-1 and the following incorporation of GR-CM-1 monomers into the GR-CM-1/GR-CM-1t heterodimers, supported additionally by the observation that the dimerization domain is retained in the truncated protein of GR-CM-1t. As for GR-CM-1t, since it had a much higher expression level than GR-CM-1, besides being incorporated into the GR-CM-1/GR-CM-1t heterodimers, the "unsaturated" GR-CM-1t should be available for the formation of homodimers; therefore, homodimers of GR-CM-1t was detected (Fig. 8B, lane 5, lower panel). Although no expected heterodimers were detected when both proteins were expressed (Fig. 8B, lane 5), we suspected that the formed heterodimers might be unstable and hence degraded or become insoluble once formed. In this *E. coli* expression system, in most cases, only monomers of tagged GR-CM-1 and GR-CM-1t proteins were detected when protein samples

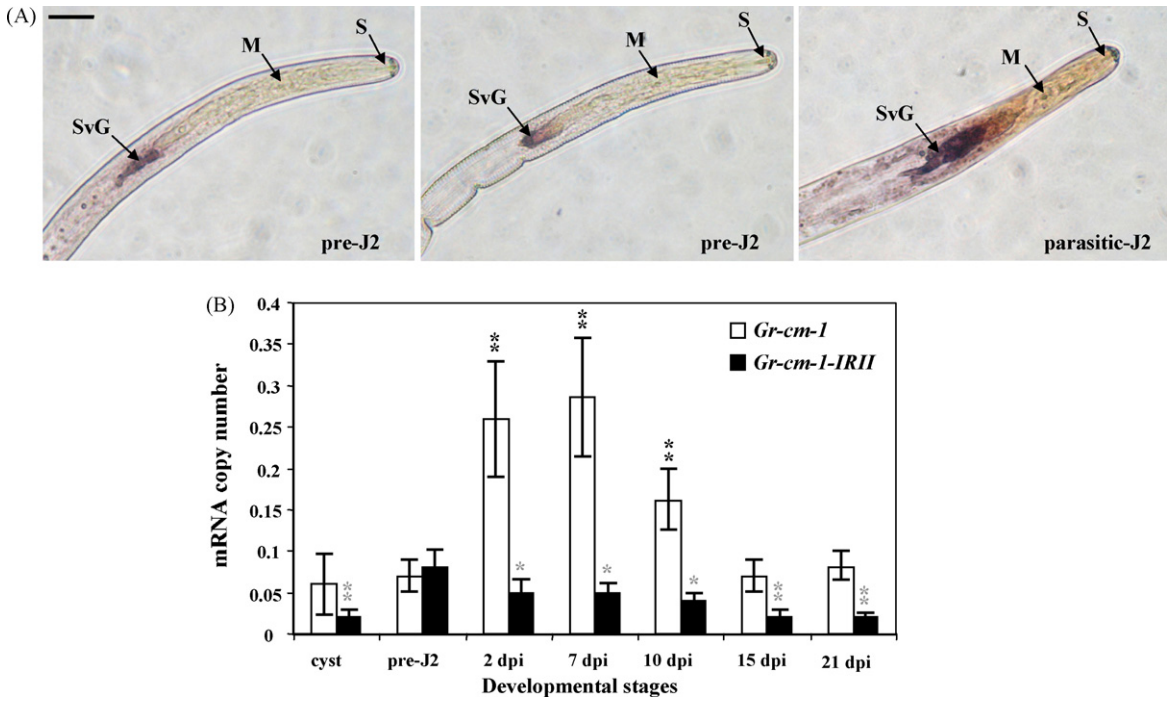

Fig. 6. Tissue localization and developmental expression of the *Gr-cm-1* gene. (A) Hybridization (dark staining) of a digoxygenin-labeled antisense *Gr-cm-1* cDNA probe (left and right panels) or a digoxygenin-labeled antisense *Gr-cm-1-IRII*-specific cDNA probe (middle panel) to corresponding transcripts accumulating exclusively within the subventral oesophageal gland cells (SvG) of a preparasitic or a parasitic second-stage juvenile of *G. rostochiensis* (Bar = 10 μm; M, metacorpus; S, stylet). (B) mRNA quantities of *Gr-cm-1* and *Gr-cm-1-IRII* in different nematode developmental stages were determined by quantitative real-time reverse transcription-PCR (qRT-PCR) using the absolute standard curve method. The calculated values were further normalized to the *Gr-act-1* gene to reveal gene expression levels in different nematode developmental stages. Each column represents the mean of two independent experiments with the standard deviations of the mean and each experiment contained three technical replicates for each mRNA sample. Asterisks ($^{*}P < 0.05$ and $^{**}P < 0.01$; *t* test) on the top of the columns indicate significant expression changes of *Gr-cm-1* and *Gr-cm-1-IRII* in nematode parasitic and cyst stages compared, respectively to those in the pre-J2 stage.

were denatured at 95C for 5 min (Fig. 8A, lane 2; Fig. 8B, lane 2, upper panel and lane 6) and basal levels of protein expression were also observed (Fig. 8B, lanes 1 and 2, lower panel, and lane 4, upper panel).

The failure in detecting the formation of GR-CM-1/GR-CM-1t heterodimers in the *E. coli* coexpression system led us to further use the yeast two-hybrid system to investigate a possible interaction between GR-CM-1 and GR-CM-1t. As expected, reporter gene (*HIS3*, *ADE2*, and *LacZ*) activation assays by growth of yeast cells cotransformed with pGBKT7–*Gr-cm-1t* and pGADT7–*Gr-cm-1* constructs on a selective SD/-Leu/-Trp/-His/-Ade plate (Fig. 8C, top middle panel) and a β-galactosidase activity assay filter paper (Fig. 8C, top right panel) revealed that GR-CM-1t and GR-CM-1 proteins could physically interact with each other in yeast, indicating that these two proteins may form heterodimers when coexpressed in the nematode. The interaction between GR-CM-1 and GR-CM-1t were confirmed to be specific as no reporter gene activation was detected by either the nutritional selection assay (Fig. 8B, second and third middle panels from the top) or the β-galactosidase activity assay (Fig. 8B, second and third right panels from the top) when the bait or prey protein was replaced with an unrelated protein (Lam or RecT). Both positive (Fig. 8C, forth panels from the top) and

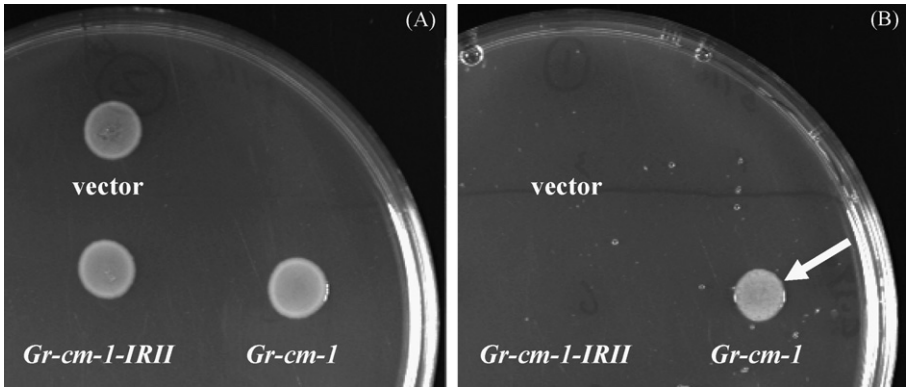

Fig. 7. Chorismate mutase (CM) complementation assay. Transformed JP2261 strains containing the pET101/D-TOPO expression vector or the construct carrying the *Gr-cm-1* cDNA or the *Gr-cm-1-IRII* cDNA were cultured on plates containing the LB medium (A) or the minimal medium without phenylalanine (B). All three transformed strains grew normally on the LB medium (A), but only the strain expressing the *Gr-cm-1* cDNA could grow on the minimal medium in the absence of phenylalanine (B, indicated by an arrow). The other two transformed strains were not able to grow on the minimal medium lacking phenylalanine (B).

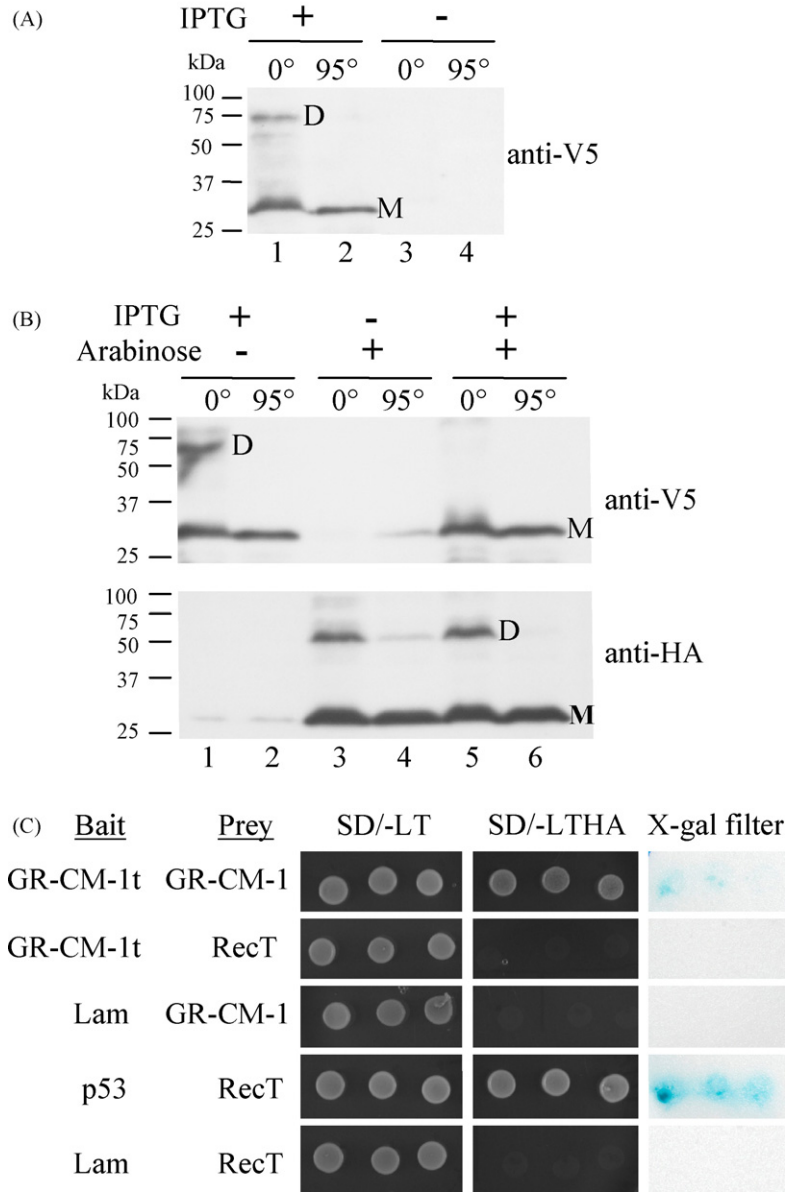

Fig. 8. Dimeric nature of GR-CM-1 and the specific interaction between GR-CM-1 and GR-CM-1t in yeast. (A) *E. coli* BL21 transformed with the V5-tagged GR-CM-1 expression construct. The expression of GR-CM-1 was induced by IPTG and detected by the anti-V5 antibody. (B) *E. coli* BL21 cotransformed with the V5-tagged GR-CM-1 and HA-tagged GR-CM-1t expression constructs and their expressions were induced individually by a single inducer (IPTG or arabinose) (lanes 1–4) or both inducers (lanes 5 and 6) as indicated. The expression of GR-CM-1t was detected by the anti-HA antibody. Before loading, soluble protein extracts were either incubated at 95 °C to disrupt dimers (lanes 2 and 4 in A, and lanes 2, 4, 6 in B) or at 0 °C to preserve dimerization (lanes 1 and 3 in A, and lanes 1, 3, 5 in B). Proteins were separated by low-temperature SDS-PAGE, and membranes were probed with indicated antibodies. Monomers (M) and homodimers (D) are labeled and positions of marker proteins are given on the left. Blots are representative of two independent experiments. (C) Yeast strain AH109 cotransformed with different combinations of bait and prey constructs (as indicated) were confirmed by growth on SD/-Leu/-Trp (SD/-LT) plates (left panels) and demonstrated activation of reporter genes of *HIS3*, *ADE2*, and *LacZ* by growth on SD/-Leu/-Trp/-His/-Ade (SD/-LTHA) plates (middle panels) and a β-galactosidase activity assay (right panels). Standard positive (p53/RecT) and negative (Lam/RecT) controls were also included. Each bait–prey combination represented three independent transformants. AH109 cotransformed with pGBKT7–*Gr-cm-1t* and pGADT7–*Gr-cm-1* could grow on SD/-LTHA plates and produced blue colors on X-gal filter similar to the positive control (second right panel from the bottom), indicating that interaction occurred between GR-CM-1t and GR-CM-1 in yeast.

negative (Fig. 8C, the bottom panels) controls included confirmed the sensitivity of the yeast two-hybrid assays. Cotransformed yeast cells were confirmed by growth on selective SD/-Leu/-Trp plates (Fig. 8C, left panels).

4. Discussion

Chorismate mutase has been found to be widely distributed in both cyst and root-knot nematode species and has been suggested to have multiple roles in modulating plant parasitism when secreted [22–24]. In this study, we cloned and characterized a new nematode *CM* gene (*Gr-cm-1*) from the potato cyst nematode *G. rostochiensis*. Most importantly, we identified two types of mRNA transcripts of the *Gr-cm-1* gene, *Gr-cm-1* and *Gr-cm-1-IRII*. *Gr-cm-1* is a fully spliced transcript whereas *Gr-cm-1-IRII* is a novel splice variant generated by retention of intron 2 of the *Gr-cm-1* pre-mRNA through alternative splicing (AS). The *Gr-cm-1* gene was further discovered to be alternatively spliced in a developmentally regulated manner. Recent advances in genome sequence and microarray studies have suggested that AS plays critical roles in regulating

and diversifying gene functions of metazoan organisms [1]. More than 70% of human genes are alternatively spliced [2] and AS is also found to play an important role in *C. elegans* development [6]. However, AS events are only observed in a few genes of animal parasitic nematodes [7,8,56]. To the best of our knowledge, this study provided the first example of AS identified in plant–parasitic nematodes.

The *Gr-cm-1* gene was found to be present as a single-copy gene in the *G. rostochiensis* genome. By extensive cloning and sequencing, PCR, and nematode genotyping analyses, the *Gr-cm-1* gene was revealed to have two alleles (*Gr-cm-1A* and *Gr-cm-1B*) in the nematode population and both alleles were found to be subjected to AS. Sequence analysis identified several putative *cis*-acting elements that may regulate AS of the *Gr-cm-1* gene. An unusual 5′ splice site of intron 2, not found in other nematode *CM* genes, was identified. Alternatively spliced exons are often found to have weak consensus 5′ or 3′ splice sites [6,57]. We speculate that this unique *cis*-acting element might affect the recognition of intron 2 in the *Gr-cm-1* pre-mRNA. Although both alleles were subjected to AS, the *Gr-cm-1B* allele appeared to have a higher intron splicing efficiency than the *Gr-cm-1A* allele. The major difference between *Gr-cm-1A* and *Gr-cm-1B* is in intron 1 where different purine-rich elements that resemble the characterized intronic splicing enhancers (ISEs) [46,47] are located. A synonymous SNP (T in *Gr-cm-1A* versus C in *Gr-cm-1B*) was also discovered in exon 3. A recent study of the human survival motor neuron (SMN) gene revealed that a single C to T transition in exon 7 affects the regulation of SMN exon 7 splicing [58]. It would be interesting to determine if differences in intron 1 and exon 3 observed between *Gr-cm-1A* and *Gr-cm-1B* regulate the splicing efficiency of intron 2.

In *H. glycines*, *Hg-cm-1* is a member of a gene family where two alleles, *Hg-cm-1A* and *Hg-cm-1B*, were identified [13]. A population genetic study showed that the *Hg-cm-1A* allele frequency was significantly increased in nematode populations grown on resistant soybean PI88788 [59]. The nematode population used in this study is a field population avirulent on potato plants carrying the *H1* resistant gene [25]. It would be interesting to determine if any of the two *Gr-cm-1* alleles is selected by resistant potato plants and if AS of *Gr-cm-1* plays a role in allele selection on resistant potatoes if such selection is revealed.

The fully spliced transcript *Gr-cm-1* encodes a full-length GR-CM-1 protein having CM enzyme activity. The restricted expression within the subventral oesophageal gland cells and the presence of a putative signal peptide in the deduced protein suggest that this nematode-produced CM is likely to be secreted into host tissue. The expression of *Gr-cm-1* was up-regulated during the onset of nematode parasitism and maintained at a relatively high level in later nematode developmental stages, indicating a potential role of GR-CM-1 in the initiation and maintenance of nematode-induced feeding sites. In agreement with this hypothesis, a recent study showed that RNAi silencing of the *CM* gene from *H. glycines* altered sexual fate that favored male development on host roots [24]. Chorismate mutases from phytonematodes have also been suggested to be involved in suppressing host defence responses and altering local phytohormone concentrations [23]. Because of the multiple functions of secreted nematode CMs in plant parasitism, silencing of *Gr-cm-1* through plant-mediated RNAi might generate novel nematode resistance in transgenic potatoes.

The *Gr-cm-1* gene was further demonstrated to be alternatively spliced in a developmentally regulated manner. The expression of *Gr-cm-1-IRII* was highest in the pre-J2 stage with a level similar to that of *Gr-cm-1*, but decreased throughout the nematode parasitic stages. Contrastingly, the expression of *Gr-cm-1* was greatly up-regulated during the onset of nematode parasitism and the magnitude of *Gr-cm-1-IRII* expression was only around 16–19% (at 7 and 2 dpi) of *Gr-cm-1* in the early parasitic stages. What might be the biological significance of this intron retention-mediated AS discovered in the *Gr-cm-1* gene? The phylogenetic relationship determined by our analysis suggested that GR-CM-1 may have a structural and enzymatic similarity to the bacterial secreted *AroQ CMs. All characterized members of the AroQ family including Mt-CM, a representative of the secreted *AroQ CMs, share a dimeric structure [42,44,50,53–55]. We propose that the full-length GR-CM-1 protein produced by *G. rostochiensis* may function as a dimeric enzyme *in planta*, supported by additional evidence that bacterial expressed GR-CM-1 can form homodimers. *Gr-cm-1-IRII*, however, contains a premature stop codon introduced by retention of intron 2 and would encode a truncated GR-CM-1t protein lacking the CM domain with no CM activity. Alternative splicing plays an important role in controlling functions and enzymatic activities of many proteins. For example, AS of the human eNOS gene generates splice variants that would produce truncated proteins lacking the reductase domain with no eNOS activity. One of the splice variants, eNOS13A, was demonstrated to form heterodimers with full-length eNOS that led to a reduction of eNOS activity by a dominant-negative effect of the truncated splice variant [37]. A truncated isoform of a pyroglutamyl aminopeptidase II (PPII) produced by AS at the exon 14-intron 14 boundary that lacked part of the C-terminal domain functioned as dominant-negative isoform by formation of heterodimers with the full-length protein and reduced PPII activity [60]. Similarly, a splice variant of the α_2 subunit of soluble guanylyl cyclase reduced α_2/β_1-catalyzed guanylyl cyclase activity by competing with the full-length α_2 subunit for dimerization with the β_1 subunit [61]. These findings have revealed a mechanism in regulation of enzyme activity by gene-rating dominant-negative splice variants through AS. The truncated GR-CM-1t protein was revealed to contain the functional dimerization domain. Because of a possible dimeric nature of the GR-CM-1 protein and the specific interaction between GR-CM-1 and GR-CM-1t demonstrated in yeast, it is likely that heterodimerization between GR-CM-1 and GR-CM-1t occurs in the nematode. GR-CM-1t lacks the CM domain and has no CM activity. Therefore, we hypothesize that GR-CM-1t functions as a dominant isoform that interferes with GR-CM-1 enzyme activity by acting through heterodimerization. Using appropriate eukaryotic expression systems as those employed for studies of AS of the *eNOS* gene [37], the *PPII* gene [60], and the guanylyl cyclase gene [61] may be necessary to further confirm this hypothesis. The higher *Gr-cm-1-IRII* mRNA/*Gr-cm-1* mRNA ratio observed in the pre-J2 stage might result in a very low level of CM activity, whereas more functional dimeric CM could be secreted *in planta* during the onset of nematode parasitism because of the dramatic decrease of the *Gr-cm-1-IRII* mRNA/*Gr-cm-1* mRNA ratio observed in the early parasitic stages. It might be worthwhile to determine if the pre-J2 nematode produces any functional CM and if GR-CM-1t could be secreted *in planta* to play a role in the initial infection process. We are attempting to generate isoform-specific antibodies to confirm the existence and the relative expression of both proteins in different nematode developmental stages and to further elucidate the functional consequence(s) of AS of *Gr-cm-1* in nematode parasitism.

Related to this study, we also identified additional alternatively spliced parasitism genes from *G. rosotchiensis* (Lu and Wang, unpublished). With the completion of several nematode genome sequencing projects, we anticipate that more alternative splicing events would be discovered that may lead to a new area of study in plant–parasitic nematodes.

Acknowledgements

We thank Prof. Afred J. Pittard for his permission to obtain the *E. coli* strain JP2261 from Dr. Richard Hussey (University of Georgia). We thank Xiaomei Deng for technical assistance, and David Thurston and Robert Oman (Cornell University) for maintaining nematode cultures. We want to extend our gratitude to Drs. Eric L. Davis (North Carolina State University), Donna M. Gibson (USDA-ARS, Biological Integrated Pest Management Research Unit, Ithaca), and Melissa G. Mitchum (University of Missouri-Columbia) for their critical reviews of the manuscript.

References

[1] Blencowe BJ. Alternative splicing: new insights from global analyses. Cell 2006;126:37–47.
[2] Johnson JM, Castle J, Garrett-Engele P, et al. Genome-wide survey of human alternative pre-mRNA splicing with exon junction microarrays. Science 2003;302:2141–4.
[3] Moroy T, Heyd F. The impact of alternative splicing in vivo: mouse models show the way. RNA 2007;13:1155–71.
[4] Lee Y, Lee Y, Kim B, et al. ECgene: an alternative splicing database update. Nucleic Acids Res 2007;35:D99–103.
[5] Iida K, Seki M, Sakurai T, et al. Genome-wide analysis of alternative pre-mRNA splicing in *Arabidopsis thaliana* based on full-length cDNA sequences. Nucleic Acids Res 2004;32:5096–103.
[6] Zahler AM. Alternative splicing in *C. elegans*. WormBook. The *C. elegans* Research Community, doi:10.1895/wormbook.1.31.1, http//www.wormbook.org. 2005.
[7] Jin J, Poole CB, Slatko BE, McReynolds LA. Alternative splicing creates sex-specific transcripts and truncated forms of the furin protease in the parasite *Dirofilaria immitis*. Gene 1999;237:161–75.
[8] Kampkotter A, Volkmann TE, de Castro SH, et al. Functional analysis of the glutathione *S*-transferase 3 from *Onchocerca volvulus* (*Ov*-GST-3): a parasite GST confers increased resistance to oxidative stress in *Caenorhabditis elegans*. J Mol Biol 2003;325:25–37.
[9] Herrmann KM. The shikimate pathway as an entry to aromatic secondary metabolism. Plant Physiol 1995;107:7–12.
[10] Dewick PM. The biosynthesis of shikimate metabolites. Natual Prod Rep 1998;15:17–58.
[11] Herrmann KM, Weaver LM. The shikimate pathway. Annu Rev Plant Physiol Plant Mol Biol 1999;50:473–503.
[12] Lambert KN, Allen KD, Sussex IM. Cloning and characterization of an esophageal-gland-specific chorismate mutase from the phytoparasitic nematode *Meloidogyne javanica*. Mol Plant Microbe Interact 1999;12:328–36.
[13] Bekal S, Niblack TL, Lambert KN. A chorismate mutase from the soybean cyst nematode *Heterodera glycines* shows polymorphisms that correlate with virulence. Mol Plant Microbe Interact 2003;16:439–46.
[14] Jones JT, Furlanetto C, Bakker E, et al. Characterization of a chorismate mutase from the potato cyst nematode *Globodera pallida*. Mol Plant Pathol 2003;4:43–50.
[15] Huang G, Dong R, Allen R, Davis EL, Baum TJ, Hussey RS. Two chorismate mutase genes from the root-knot nematode *Meloidogyne incognita*. Mol Plant Pathol 2005;6:23–30.
[16] Long H, Wang X, Xu J. Molecular cloning and life-stage expression pattern of a new chorismate mutase gene from the root-knot nematode *Meloidogyne arenaria*. Plant Pathol 2006;55:559–63.
[17] Long H, Wang X, Xu JH, Hu YJ. Isolation and characterization of another cDNA encoding a chorismate mutase from the phytoparasitic nematode *Meloidogyne arenaria*. Exp Parasitol 2006;113:106–11.
[18] Haslam E. Shikimic acid: metabolism and metabolites. New York: John Wiley & Sons; 1993.
[19] Weaver LM, Herrmann KM. Dynamics of the shikimate pathway in plants. Trends Plant Sci 1997;2:346–51.
[20] Hussey RS. Disease-inducing secretions of plant–parasitic nematodes. Annu Rev Phytopathol 1989;27:123–41.
[21] Davis EL, Hussey RS, Baum TJ, et al. Nematode parasitism genes. Annu Rev Phytopathol 2000;38:365–96.
[22] Davis EL, Hussey RS, Baum TJ. Getting to the roots of parasitism by nematodes. Trends Parasitol 2004;20:134–41.
[23] Doyle EA, Lambert KN. *Meloidogyne javanica* chorismate mutase 1 alters plant cell development. Mol Plant Microbe Interact 2003;16:123–31.
[24] Bakhetia M, Urwin PE, Atkinson HJ. qPCR analysis and RNAi define pharyngeal gland cell-expressed genes of *Heterodera glycines* required for initial interactions with the host. Mol Plant Microbe Interact 2007;20:306–12.
[25] Brodie BB. Classical and molecular approaches for managing nematodes affecting potato. Can J Plant Pathol 1999;21:222–30.
[26] Skantar AM, Handoo ZA, Carta LK, Chitwood DJ. Morphological and molecular identification of *Globodera pallida* associated with potato in Idaho. J Nematol 2007;39:133–44.
[27] Sun F, Miller S, Wood S, Cote M-J. Occurrence of potato cyst nematode, *Globodera rostochiensis*, on potato in the Saint-Amable region, Quebec, Canada. Plant Dis 2007;91:908.
[28] Brodie BB, Plaisted RL, de Scurrah MM. The incorporation of resistance to *Globodera pallida* into *Solanum tuberosum* germplasm adapted to North America. Am Potato J 1991;68:1–11.
[29] Brodie BB. Effect of initial nematode density on managing *Globodera rostochiensis* with resistant cultivars and nonhosts. J Nematol 1996;28:510–9.
[30] Clarke AJ, Perry RN. Hatching of cyst-nematodes. Nematologica 1977;23:350–68.
[31] Edwards K, Johnstone C, Thompson C. A simple and rapid method for the preparation of plant genomic DNA for PCR analysis. Nucleic Acids Res 1991;19:1349.
[32] Sambrook J, Fritsch EF, Maniatis T. Molecular cloning: a laboratory manual. 2nd ed. Cold Spring Harbor, New York: Cold Spring Harbor Laboratory Press; 1989.
[33] Wang X, Allen R, Ding X, et al. Signal peptide-selection of cDNA cloned directly from the esophageal gland cells of the soybean cyst nematode *Heterodera glycines*. Mol Plant-Microbe Interact 2001;14:536–44.
[34] De Boer JM, Yan Y, Smant G, Davis EL, Baum TJ. In-situ hybridization to messenger RNA of *Heterodera glycines*. J Nematol 1998;30:309–12.
[35] Baldwin GS, Davidson BE. A kinetic and structural comparison of chorismate mutase/prephenate dehydratase from mutant strains of *Escherichia coli* K 12 defective in the *PheA* gene. Arch Biochem Biophys 1981;211:66–75.
[36] Venema RC, Ju H, Zou R, Ryan JW, Venema VJ. Subunit interactions of endothelial nitric-oxide synthase. Comparisons to the neuronal and inducible nitric-oxide synthase isoforms. J Biol Chem 1997;272:1276–82.
[37] Lorenz M, Hewing B, Hui J, et al. Alternative splicing in intron 13 of the human eNOS gene: a potential mechanism for regulating eNOS activity. FASEB J 2007;21:1556–64.
[38] Altschul SF, Madden TL, Schaffer AA, et al. Gapped BLAST and PSI-BLAST: a new generation of protein database search programs. Nucleic Acids Res 1997;25:3389–402.
[39] Marchler-Bauer A, Bryant SH. CD-Search: protein domain annotations on the fly. Nucleic Acids Res 2004;32:W327–31.
[40] Nielsen H, Engelbrecht J, Brunak S, von Heijne G. Identification of prokaryotic and eukaryotic signal peptides and prediction of their cleavage sites. Protein Eng 1997;10:1–6.
[41] Thompson JD, Gibson TJ, Plewniak F, Jeanmougin F, Higgins DG. The CLUSTAL_X windows interface: flexible strategies for multiple sequence alignment aided by quality analysis tools. Nucleic Acids Res 1997;25:4876–82.
[42] Qamra R, Prakash P, Aruna B, Hasnain SE, Mande SC. The 2.15 Å crystal structure of *Mycobacterium tuberculosis* chorismate mutase reveals an unexpected gene duplication and suggests a role in host–pathogen interactions. Biochemistry 2006;45:6997–7005.
[43] Felsenstein J. PHYLIP—Phylogeny Inference Package (Version 3.2). Cladistics 1989;5:164–6.
[44] Lee AY, Karplus PA, Ganem B, Clardy J. Atomic structure of the buried catalytic pocket of *Escherichia coli* chorismate mutase. J Am Chem Soc 1995;117:3627–8.
[45] Blumenthal T, Steward K. RNA processing and gene structure. In: Riddle DL, Blumenthal T, Meyer BJ, Priess JR, editors, *C. elegans* II. Cold Spring Harbor, New York: Cold Spring Harbor Laboratory Press; 1997. p. 117–46.
[46] Hastings ML, Wilson CM, Munroe SH. A purine-rich intronic element enhances alternative splicing of thyroid hormone receptor mRNA. RNA 2001;7:859–74.
[47] Mercado PA, Ayala YM, Romano M, Buratti E, Baralle FE. Depletion of TDP 43 overrides the need for exonic and intronic splicing enhancers in the human apoA-II gene. Nucleic Acids Res 2005;33:6000–10.
[48] Xia T, Song J, Zhao G, Aldrich H, Jensen RA. The *AroQ*-encoded monofunctional chorismate mutase (CM-F) protein is a periplasmic enzyme in *Erwinia herbicola*. J Bacteriol 1993;175:4729–37.
[49] Calhoun DH, Bonner CA, Gu W, Xie G, Jensen RA. The emerging periplasm-localized subclass of AroQ chorismate mutases, exemplified by those from *Salmonella typhimurium* and *Pseudomonas aeruginosa*. Genome Biol 2001;2:1–16.
[50] Sasso S, Ramakrishnan C, Gamper M, Hilvert D, Kast P. Characterization of the secreted chorismate mutase from the pathogen *Mycobacterium tuberculosis*. FEBS J 2005;272:375–89.
[51] Takai S, Hines SA, Sekizaki T, et al. DNA sequence and comparison of virulence plasmids from *Rhodococcus equi* ATCC 33701 and 103. Infect Immun 2000;68:6840–7.
[52] Bumann D. Examination of *Salmonella* gene expression in an infected mammalian host using the green fluorescent protein and two-colour flow cytometry. Mol Microbiol 2002;43:1269–83.
[53] Xue Y, Lipscomb WN, Graf R, Schnappauf G, Braus G. The crystal structure of allosteric chorismate mutase at 2.2-Å resolution. Proc Natl Acad Sci U S A 1994;91:10814–8.
[54] Strater N, Schnappauf G, Braus G, Lipscomb WN. Mechanisms of catalysis and allosteric regulation of yeast chorismate mutase from crystal structures. Structure 1997;5:1437–52.
[55] Okvist M, Dey R, Sasso S, Grahn E, Kast P, Krengel U. 1.6 Å crystal structure of the secreted chorismate mutase from *Mycobacterium tuberculosis*: novel fold topology revealed. J Mol Biol 2006;357:1483–99.
[56] Crossgrove K, Laudet V, Maina CV. *Dirofilaria immitis* encodes *Di-nhr-7*, a putative orthologue of the *Drosophila* ecdysone-regulated *E78* gene. Mol Biochem Parasitol 2002;119:169–77.

[57] Michael IP, Kurlender L, Memari N, et al. Intron retention: a common splicing event within the human kallikrein gene family. Clin Chem 2005;51:506–15.
[58] Miyaso H, Okumura M, Kondo S, Higashide S, Miyajima H, Imaizumi K. An intronic splicing enhancer element in survival motor neuron (SMN) pre-mRNA. J Biol Chem 2003;278:15825–31.
[59] Lambert KN, Bekal S, Domier LL, Niblack TL, Noel GR, Smyth CA. Selection of *Heterodera glycines chorismate mutase-1* alleles on nematode-resistant soybean. Mol Plant Microbe Interact 2005;18:593–601.
[60] Chavez-Gutierrez L, Bourdais J, Aranda G, et al. A truncated isoform of pyroglutamyl aminopeptidase II produced by exon extension has dominant-negative activity. J Neurochem 2005;92:807–17.
[61] Behrends S, Harteneck C, Schultz G, Koesling D. A variant of the α_2 subunit of soluble guanylyl cyclase contains an insert homologous to a region within adenylyl cyclases and functions as a dominant negative protein. J Biol Chem 1995;270:21109–13.